PFC/JA-86-54

INFLUENCE OF UNTRAPPED ELECTRONS ON THE SIDEBAND INSTABILITY IN A HELICAL WIGGLER FREE ELECTRON LASER

Ronald C. Davidson

and

Jonathan S. Wurtele

September, 1986

Plasma Fusion Center
Massachusetts Institute of Technology
Cambridge, Massachusetts 02139

INFLUENCE OF UNTRAPPED ELECTRONS ON THE SIDEBAND INSTABILITY IN A HELICAL WIGGLER FREE ELECTRON LASER

Ronald C. Davidson[†]
Science Applications International Corporation, Boulder, CO 80302

Jonathan S. Wurtele
Plasma Fusion Center, Massachusetts Institute of Technology, Cambridge, MA 02139

ABSTRACT

The detailed influence of an untrapped-electron population on the sideband instability in a helical wiggler free electron laser is investigated for small-amplitude perturbations about a constant-amplitude ($\hat{a}_s^0$ = const.) primary electromagnetic wave with slowly varying equilibrium phase δ_s^0. A simple model is adopted in which all of the trapped electrons are deeply trapped, and the equilibrium motion of the untrapped electrons (assumed monoenergetic) is only weakly modulated by the ponderomotive potential. The theoretical model is based on the single-particle orbit equations together with Maxwell's equations and appropriate statistical averages. Moreover, the stability analysis is carried out in the ponderomotive frame, which leads to a substantial simplification in deriving the dispersion relation. Detailed stability properties are investigated over a wide range of dimensionless pump strength $\Omega_B/\Gamma_b ck_0$ and fraction of untrapped electrons $f_u = \hat{n}_u/\hat{n}_b$. When both trapped and untrapped electrons are present, there are generally two types of unstable modes, referred to as the sideband mode, and the untrapped-electron mode. For $f_u = 0$, only the sideband instability is present. As f_u is increased, the growth rate of the sideband instability decreases, whereas the growth rate of the untrapped-electron mode increases until only the untrapped-electron mode is unstable for $f_u = 1$. It is found that the characteristic maximum growth rate of the most unstable mode varies by only a small amount over the entire range of f_u from $f_u = 0$ (no untrapped electrons) to $f_u = 1$ (no trapped electrons). This suggests that it is a serious oversight to neglect an untrapped-electron component when calculating the detailed linear and nonlinear evolution of the beam electrons and the radiation field.

[†] Permanent address: Plasma Fusion Center, Massachusetts Institute of Technology, Cambridge, MA 02139.

I. INTRODUCTION AND SUMMARY

Free electron lasers (FELs),[1-4] as evidenced by the growing experimental[5-22] and theoretical[23-70] literature on this subject, can be effective sources for coherent radiation generation by intense relativistic electron beams. Recent theoretical studies have included investigations of nonlinear effects[23-47] and saturation mechanisms, the influence of finite geometry on linear stability properties,[48-53] novel magnetic field geometries for radiation generation,[48,54-58] and fundamental studies of stability behavior.[59-70] One topic of considerable practical interest is the sideband instability[36] which results from the bounce motion of electrons trapped in the (finite-amplitude) ponderomotive potential. Both kinetic[23-25] and single-particle[36-47] models of the sideband instability have been developed, and numerical simulations[39-47] have been carried out. However, with the exception of the recent kinetic formalism developed by Davidson et al.,[23-25] the analytical treatments have consistently neglected the effects of any untrapped-electron population.

The purpose of the present analysis is to investigate the detailed influence of untrapped electrons on the sideband instability. Small-amplitude perturbations are assumed about a constant-amplitude ($\hat{a}_s^0$ = const.) primary electromagnetic wave with slowly varying equilibrium phase δ_s^0. Moreover, we adopt a simple model in which all of the trapped electrons are deeply trapped, and the equilibrium motion of the untrapped electrons (assumed monoenergetic) is only weakly modulated by the ponderomotive potential. The theoretical model (Sec. II) is based on the single-particle orbit equations together with Maxwell's equations and appropriate statistical averages.[36,37] Like our recent treatment[37] of the sideband instability

(which neglects the effects of untrapped electrons), the present analysis is carried out in the ponderomotive frame, which leads to a substantial simplification in the analysis.

The theoretical model and assumptions are described in Sec. II. A tenuous, relativistic electron beam propagates through a constant-amplitude helical wiggler magnetic field with wavelength $\lambda_0 = 2\pi/k_0 = \text{const.}$, normalized amplitude $a_w = e\hat{B}_w/mc^2k_0 = \text{const.}$, and vector potential specified by [Eq.(1)]

$$\underset{\sim}{A}_w(\underset{\sim}{x}) = -\frac{mc^2}{e}\, a_w\left(\cos k_0 z\hat{\underset{\sim}{e}}_x + \sin k_0 z\hat{\underset{\sim}{e}}_y\right) \quad .$$

The model neglects longitudinal perturbations (Compton-regime approximation with $\delta\phi \simeq 0$) and transverse spatial variations ($\partial/\partial x = 0 = \partial/\partial y$). Moreover, the analysis is carried out for the case of finite-amplitude primary electromagnetic wave (ω_s, k_s) with right-circular polarization and vector potential specified by [Eq.(2)]

$$\underset{\sim}{A}_s(\underset{\sim}{x},t) = \frac{mc^2}{e}\,\hat{a}_s(z,t)\left\{\cos[k_s z - \omega_s t + \delta_s(z,t)]\hat{\underset{\sim}{e}}_x\right.$$

$$\left. - \sin[k_s z - \omega_s t + \delta_s(z,t)]\hat{\underset{\sim}{e}}_y\right\} \quad ,$$

where the normalized amplitude $\hat{a}_s(z,t)$ and wave phase $\delta_s(z,t)$ are treated as slowly varying (Eikonal approximation). A detailed investigation of the sideband instability simplifies considerably if the analysis is carried out in the ponderomotive frame[37,71,72] moving with velocity [Eq.(3)]

$$v_p = \frac{\omega_s}{k_s + k_0} \quad .$$

In the ponderomotive frame ("primed" variables), the nonlinear evolution of $\hat{a}_s(z',t')$ and $\delta_s'(z',t')$ is described by Eqs.(5) and (6). Here, correct to lowest order in $|(\omega_s'\hat{a}_s)^{-1}(\partial\hat{a}_s/\partial t')| \ll 1$, energy is conserved in the ponderomotive frame ($d\gamma_j'/dt' = 0$), and the axial orbit $\theta_{js}'(t') = k_p'z_j'(t')$ solves Eq.(13), where $k_p' = (k_s + k_0)/\gamma_p$ is the wavenumber of the ponderomotive potential, and $\gamma_p = (1 - v_p^2/c^2)^{-\frac{1}{2}}$. Moreover, the real oscillation frequency ω_s' and wavenumber k_s' are related by the dispersion relation (7). In obtaining Eqs.(5), (6), (7), and (13), it is assumed that all electrons have zero transverse canonical momentum, i.e., $P_{xj}' = 0 = P_{yj}'$.

In Sec. III, Eqs.(5), (6) and (13) are used to investigate the influence of untrapped electrons on the sideband instability for small-amplitude perturbations about a primary electromagnetic wave with constant amplitude $\hat{a}_s^0 = $ const. (independent of z' and t'). The trapped and untrapped electrons are treated as distinct components. Moreover, the principal assumptions in the present analysis are the following (Sec. III.A).

(a) All of the trapped electrons are <u>deeply</u> trapped with a sharply defined energy $\gamma_j' = \hat{\gamma}_T' \simeq \hat{\gamma}_-' = [1 + (a_w - \hat{a}_s^0)^2]^{\frac{1}{2}}$. This implies that the trapped electrons are spatially localized ("bunched") near the bottom of the ponderomotive potential (Fig. 2). The average density of the trapped electrons in the ponderomotive frame is $\hat{n}_T' = \hat{n}_T/\gamma_p$.

(b) All of the untrapped electrons have a sharply defined energy $\gamma_j' = \hat{\gamma}_u' > \hat{\gamma}_+' = [1 + (a_w + \hat{a}_s^0)^2]^{\frac{1}{2}}$, where $\hat{\gamma}_u'$ is sufficiently large that the motion of the untrapped electrons is only weakly modulated by the ponderomotive potential (Fig. 2). The average density of the untrapped electrons in the ponderomotive frame is $\hat{n}_u' = \hat{n}_u/\gamma_p$.

(c) Consistent with (a) and (b), we assume that the perturbations are about a quasi-steady equilibrium state characterized by $\hat{a}_s^0 = $ const.

(independent of z' and t') and $\partial\delta_s^0/\partial t' = 0$. However, a slow spatial variation of the equilibrium phase δ_s^0 is required [Eq.(41)]

Following a discussion of the quasi-steady equilibrium state (Sec. III.B), we analyse the linearized wave and particle orbit equations (Sec. III.C), and derive the dispersion relation (70) for small-amplitude perturbations in the ponderomotive frame (Sec. III.D). Here, it is assumed that the perturbed amplitude $\delta\hat{a}_s(z',t')$, the perturbed phase $\tilde{\delta}_s'(z',t')$, etc., vary as

$$\exp\left\{-i(\Delta\omega')t' + i(\Delta k')z'\right\}$$

where $\mathrm{Im}(\Delta\omega') > 0$ corresponds to instability (temporal growth). The dispersion relation (70) relates $\Delta\omega'$ to $\Delta k'$ and other system parameters such as $\hat{a}_s^0$, k_p', $\hat{n}_T'$, $\hat{n}_u'$, etc.

Finally, in Sec. IV, the dispersion relation (70) is used to investigate detailed properties of the sideband instability including the effects of the untrapped electrons. First, we transform Eq.(70) back to the laboratory-frame frequency $\omega = \omega_s + \Delta\omega$ and wavenumber $k = k_s + \Delta k$ making use of the transformation in Eq.(71) relating $(\Delta\omega,\Delta k)$ to $(\Delta\omega',\Delta k')$. In this regard, it is convenient to introduce the shorthand notation [Eq.(73)]

$$\Delta\Omega = \Delta\omega - v_p\Delta k \ ,$$

$$\Delta K = k_0 \frac{v_p}{c} \frac{\Delta k}{k_s} \ ,$$

where $v_p = \omega_s/(k_s + k_0)$, and (ω_s,k_s) are the frequency and wavenumber of the primary electromagnetic wave in the laboratory frame. After some algebraic manipulation (Sec. IV.A), it is straightforward to show that the dispersion relation (70) can be expressed in the equivalent form [Eq.(80)]

$$1 - \frac{\Omega_B^2}{(\Delta\Omega)^2} - \frac{4\Omega_B^2(\Gamma_T ck_0/\Omega_B)^6}{(\Delta\Omega - c\Delta K)^2}$$

$$= \alpha_u \frac{(\Gamma_T ck_0)^3[(\Delta\Omega)^2 - \Omega_B^2]}{(\Delta\Omega)^2(\Delta\Omega - c\Delta K)^2[(\Delta\Omega)^2 - \hat{\beta}_u'^2 c^2 k_0^2]^2}$$

$$\times \left\{ \alpha_u(\Gamma_T ck_0)^3 + 4(\Delta\Omega)(\Delta\Omega - c\Delta K)\hat{\beta}_u' ck_0 \right.$$

$$\left. + 2(\Gamma_T ck_0)\left(\frac{\Gamma_T ck_0}{\Omega_B}\right)^2[(\Delta\Omega)^2 + \hat{\beta}_u'^2 c^2 k_0^2]\left[1 + \frac{(\Delta\Omega)^2}{(\Delta\Omega)^2 - \Omega_B^2}\right]\right\} .$$

In Eq.(80), $\alpha_u = (\hat{n}_u'/\hat{n}_T')(\hat{\gamma}_-'/\hat{\gamma}_u')^3$ [Eq.(75)] is a measure of the ratio of the untrapped electron density to the trapped electron density, and $\hat{\beta}_u' = (1 + v_p/c)\beta_u'$ [Eq.(78)] is proportional to the speed of the untrapped electrons in the ponderomotive frame. Moreover, Ω_B is the bounce frequency of deeply trapped electrons defined by [Eq(24)]

$$\Omega_B = \left(1 + \frac{v_p}{c}\right)\left(\frac{a_w \hat{a}_s^0}{1 + a_w^2}\right)^{\frac{1}{2}} ck_0$$

in the laboratory frame, and Γ_T is the (small) dimensionless gain parameter defined by [Eq.(81)]

$$\Gamma_T^3 = \frac{1}{4} \frac{a_w^2}{(1 + a_w^2)^{3/2}} \frac{(4\pi\hat{n}_T e^2/m)}{\gamma_p^3 c^2 k_0^2} \frac{(1 + v_p/c)}{v_p/c} << 1 ,$$

where use has been made of $\hat{n}_T' = \hat{n}_T/\gamma_p$. Consistent with Assumption (b) at the beginning of Sec. III, we require that $\hat{\beta}_u' ck_0$ be sufficiently large in comparison with Ω_B in Eq.(80) in order that the untrapped-electron motion be only weakly modulated by the ponderomotive potential (Fig. 2).

Equation (86), which is equivalent to Eq.(80), constitutes the final dispersion relation which is analysed numerically in Sec. IV.B. For $f_u = \hat{n}_u/\hat{n}_b = 0$, which corresponds to no untrapped electrons ($\hat{n}_u = 0$), Eq.(86) is the familiar dispersion relation for the sideband instability[37,73] in circumstances where the equilibrium wave phase is slowly varying [Eq.(41)]. For $f_u \neq 0$, however, it is found that the untrapped electrons can significantly modify stability behavior (Sec. IV.B). Detailed stability properties are investigated over a wide range of dimensionless pump strength $\Omega_B/\Gamma_b ck_0$ (where $\Gamma_b^3 = \hat{n}_b \Gamma_T^3/\hat{n}_T$) and fraction of untrapped electrons $f_u = \hat{n}_u/\hat{n}_b$. When both trapped and untrapped electrons are present, there are generally two types of unstable modes, referred to as the sideband mode, and the untrapped-electron mode. For $f_u = 0$, only the sideband instability is present. As f_u is increased, the growth rate of the sideband instability decreases, whereas the growth rate of the untrapped-electron mode increases until only the untrapped-electron mode is unstable for $f_u = 1$.

The present analysis indicates that the detailed properties of $\mathrm{Im}(\Delta\Omega)/\Gamma_b ck_0$ versus $\Delta K/\Gamma_b k_0$ are quite different for the two unstable modes. Equally important, however, it is found that the characteristic maximum growth rate of the most unstable mode varies by only a small amount over the entire range of f_u from $f_u = 0$ (no untrapped electrons) to $f_u = 1$ (no trapped electrons).

II. THEORETICAL MODEL AND ASSUMPTIONS

A. Basic Equations and Assumptions

A tenuous, relativistic electron beam propagates in the z-direction through a constant-amplitude helical wiggler magnetic field with wavelength $\lambda_0 = 2\pi/k_0 = \text{const.}$, normalized amplitude $a_w = e\hat{B}_w/mc^2k_0 = \text{const.}$, and vector potential specified by

$$\underset{\sim}{A}_w(\underset{\sim}{x}) = -\frac{mc^2}{e}\, a_w\left(\cos k_0 z\hat{\underset{\sim}{e}}_x + \sin k_0 z\hat{\underset{\sim}{e}}_y\right) \quad . \tag{1}$$

The model neglects longitudinal perturbations (Compton-regime approximation, $\delta\phi \simeq 0$) and transverse spatial variations ($\partial/\partial x = 0 = \partial/\partial y$). Moreover, the analysis is carried out for the case of a finite-amplitude primary electromagnetic wave (ω_s, k_s) with right-circular polarization and vector potential specified by[37]

$$\underset{\sim}{A}_s(\underset{\sim}{x},t) = \frac{mc^2}{e}\,\hat{a}_s(z,t)\Big\{\cos[k_s z - \omega_s t + \delta_s(z,t)]\hat{\underset{\sim}{e}}_x - \sin[k_s z - \omega_s t + \delta_s(z,t)]\hat{\underset{\sim}{e}}_y\Big\} \quad , \tag{2}$$

where the normalized amplitude $\hat{a}_s(z,t)$ and wave phase $\delta_s(z,t)$ are treated as slowly varying (Eikonal approximation). Here, -e is the electron charge, m is the electron rest mass, and c is the speed of light in vacuo. In Eqs.(1) and (2), the wiggler magnetic field is determined from $\underset{\sim}{B}_w = \nabla \times \underset{\sim}{A}_w$, and the electromagnetic wave field is determined from $\underset{\sim}{B}_s = \nabla \times \underset{\sim}{A}_s$ and $\underset{\sim}{E}_s = -c^{-1}\partial\underset{\sim}{A}_s/\partial t$. A detailed investigation of the sideband instability simplifies considerably if the analysis is carried out in the ponderomotive frame moving with velocity[37,71,72]

$$v_p = \frac{\omega_s}{k_s + k_0} \ . \tag{3}$$

Therefore, the present analysis is carried out in ponderomotive-frame variables (z',t',γ') defined by the Lorentz transformation

$$\begin{aligned} z' &= \gamma_p(z - v_p t) \ , \\ t' &= \gamma_p(t - v_p z/c^2) \ , \\ \gamma' &= \gamma_p(\gamma - v_p p_z/mc^2) \ , \end{aligned} \tag{4}$$

where $\gamma_p = (1 - v_p^2/c^2)^{-\frac{1}{2}}$, $\gamma' mc^2 = (m^2c^4 + c^2p_x'^2 + c^2p_y'^2 + c^2p_z'^2)^{\frac{1}{2}}$ is the mechanical energy, and the components of momentum (p_x',p_y',p_z') are related to the velocity $\underset{\sim}{v}' = d\underset{\sim}{x}'/dt'$ by $\underset{\sim}{p}' = \gamma' m \underset{\sim}{v}'$.

In the ponderomotive frame, the slow nonlinear evolution of $\hat{a}_s(z',t')$ and $\delta_s'(z',t')$ is described by[37]

$$2\omega_s' \left(\frac{\partial}{\partial t'} + \frac{k_s'c^2}{\omega_s'} \frac{\partial}{\partial z'} \right) \hat{a}_s = \frac{4\pi e^2 a_w}{m} \frac{1}{L'} \left\langle \sum_j \frac{\sin(\theta_{js}' + \delta_s')}{\gamma_j'} \right\rangle \ , \tag{5}$$

$$2\omega_s' \hat{a}_s \left(\frac{\partial}{\partial t'} + \frac{k_s'c^2}{\omega_s'} \frac{\partial}{\partial z'} \right) \delta_s' = \frac{4\pi e^2 a_w}{m} \frac{1}{L'} \left\langle \sum_j \frac{\cos(\theta_{js}' + \delta_s')}{\gamma_j'} \right\rangle \ , \tag{6}$$

where the real oscillation frequency ω_s' and wavenumber k_s' are related by the dispersion relation[37]

$$\omega_s'^2 = c^2 k_s'^2 + \frac{4\pi e^2}{m} \frac{1}{L'} \left\langle \sum_j \frac{1}{\gamma_j'} \right\rangle \ . \tag{7}$$

In Eqs.(5)-(7), $\left\langle \sum_j \cdots \right\rangle$ denotes statistical average, and the axial orbit $\theta_{js}'(t') = k_p' z_j'(t')$ and energy $\gamma_j'(t')$ of the j'th electron solve[37]

$$\frac{d^2}{dt'^2}\theta'_{js} + \frac{c^2 k'^2_p a_w}{\gamma'^2_j}\,\mathrm{Im}\left[\hat{a}_s \exp(i\theta'_{js} + i\delta'_s)\right]$$

$$= \frac{c^2 k'_p a_w}{\gamma'^2_j}\,\mathrm{Re}\left\{\exp(i\theta'_{js})\left(\frac{\partial}{\partial z'_j} + \frac{1}{c^2}\frac{dz'_j}{dt'}\frac{\partial}{\partial t'}\right)\left[\hat{a}_s \exp(i\delta'_s)\right]\right\}, \tag{8}$$

and

$$\frac{d}{dt'}\gamma'_j = -\frac{a_w}{\gamma'_j}\,\mathrm{Re}\left\{\frac{\partial}{\partial t'}\left[\hat{a}_s \exp(i\delta'_s)\right]\right\}. \tag{9}$$

In Eqs.(8) and (9), $k'_p = (k_s + k_0)/\gamma_p$ is the wavenumber of the ponderomotive potential, and γ'_j is defined by

$$\gamma'^2_j = 1 + \frac{p'^2_{zj}}{m^2c^2} + a_w^2 + \hat{a}_s^2 - 2a_w \mathrm{Re}\left[\hat{a}_s \exp(i\theta'_{js} + i\delta'_s)\right] \tag{10}$$

in the ponderomotive frame. In obtaining Eqs.(8) and (9) from $dp'_{zj}/dt' = -mc^2 \partial\gamma'_j/\partial z'_j$ and $d\gamma'_j/dt' = \partial\gamma'_j/\partial t'$, we have neglected $\hat{a}_s^2 << 1 + a_w^2$ in Eq.(10). Moreover, it is assumed that all electrons have zero transverse canonical momentum, i.e., $P'_{xj} = 0 = P'_{yj}$.

There is some latitude in specifying the precise operational meaning[36] of the statistical averages $\left\langle \sum_j \cdots \right\rangle$ occurring in Eqs.(5)-(7). For present purposes, let us assume that the orbits $z'_j(t')$ and $\gamma'_j(t')$ have been calculated from Eqs.(8) and (9) in terms of the initial values $z'_j(0)$ and $\gamma'_j(0)$. Then the simplest definition of the statistical average $\left\langle \sum_j \cdots \right\rangle$ over some phase function $\psi\left(\theta'_{js}(0), \gamma'_j(0)\right)$ is given by

$$\frac{1}{L'}\left\langle \sum_j \psi\left(\theta'_{js}(0), \gamma'_j(0)\right)\right\rangle$$

$$= \hat{n}'_b \int_0^{2\pi} \frac{d\theta'_0}{2\pi} \int_1^{\infty} d\gamma'_0 G(\theta'_0, \gamma'_0)\psi(\theta'_0, \gamma'_0). \tag{11}$$

Here, $\hat{n}_b'$ is the average density of the beam electrons in the ponderomotive frame, and $G(\theta_0', \gamma_0')$ is the (probability) distribution of electrons in initial phase θ_0' and energy γ_0'. Moreover, $L' = 2\pi/k_p'$ is the basic periodicity length in the ponderomotive frame.

Equations (5)-(9) constitute a closed description of the nonlinear evolution of the system. In this regard, further simplification of Eqs. (8) and (9) is possible by virtue of the assumption of slowly varying wave amplitude and phase (Eikonal approximation), i.e.,

$$|\omega_s'| >> \left|\left[\hat{a}_s \exp(i\delta_s')\right]^{-1} \frac{\partial}{\partial t'} \left[\hat{a}_s \exp(i\delta_s')\right]\right| ,$$
$$|k_s'| >> \left|\left[\hat{a}_s \exp(i\delta_s')\right]^{-1} \frac{\partial}{\partial z'} \left[\hat{a}_s \exp(i\delta_s')\right]\right| . \qquad (12)$$

In particular, to lowest order, it is valid to neglect the local time and spatial derivatives on the right-hand sides of Eqs.(8) and (9). This gives the approximate dynamical equations[37]

$$\frac{d^2}{dt'^2} \theta_{js}' + \frac{c^2 k_p'^2 a_w}{\gamma_j'^2} \mathrm{Im}\left[\hat{a}_s \exp(i\theta_{js}' + i\delta_s')\right] = 0 , \qquad (13)$$

$$\frac{d}{dt'} \gamma_j' = 0 . \qquad (14)$$

The major benefit of carrying out the analysis in the ponderomotive frame is evident from Eqs.(13) and (14). To lowest order, the particle energy γ_j' can be treated as constant in Eqs.(5)-(7) and (13).

In the subsequent analysis, we make use of the closed description of the nonlinear evolution of the system provided by Eqs.(5)-(7) and Eqs.(13) and (14).

B. Definitions and Notation

For future reference, in this section we establish the basic definitions and notation to be used in the stability analysis in Secs. III and IV.

The wave frequency and wavenumber (ω',k') in the ponderomotive frame are related to the wave frequency and wavenumber (ω,k) in the laboratory frame by

$$\begin{aligned} \omega' &= \gamma_p(\omega - kv_p) \ , \\ k' &= \gamma_p(k - \omega v_p/c^2) \ , \end{aligned} \tag{15}$$

where $v_p = \omega_s/(k_s + k_0)$ and $\gamma_p = (1 - v_p^2/c^2)^{-\frac{1}{2}}$. As a special case, we obtain $\omega_s' = \gamma_p(\omega_s - k_s v_p)$ from Eq.(15), which gives

$$\omega_s' = \gamma_p k_0 v_p \ . \tag{16}$$

In the present analysis, it is also assumed that the electron beam is sufficiently tenuous that beam dielectric effects can be neglected in the dispersion relation (7) (and its laboratory-frame analogue). This gives the vacuum dispersion relation $\omega_s'^2 = c^2 k_s'^2$, or equivalently $\omega_s^2 = c^2 k_s^2$, for the primary electromagnetic wave. Assuming a forward-moving electromagnetic wave, we solve the simultaneous resonance conditions

$$\begin{aligned} \omega_s &= +ck_s \ , \\ \omega_s &= (k_s + k_0)v_p \ , \end{aligned} \tag{17}$$

for ω_s and k_s. This readily gives the familiar results[37]

$$\begin{aligned} \omega_s &= \gamma_p^2(1 + v_p/c)k_0 v_p \ , \\ k_s &= \gamma_p^2(1 + v_p/c)(v_p/c)k_0 \ , \end{aligned} \tag{18}$$

where $\gamma_p^2 = (1 - v_p^2/c^2)^{-\frac{1}{2}}$, and $v_p = \omega_s/(k_s + k_0)$ is (nearly) synchronous with the average axial velocity V_b of the beam electrons. Moreover, from Eq.(18), the ponderomotive wavenumber $k_p' = (k_s + k_0)/\gamma_p$ can be expressed as

$$k_p' = \gamma_p(1 + v_p/c)k_0 \ . \tag{19}$$

In circumstances where perturbations are about a primary electromagnetic wave with amplitude $\hat{a}_s^0$ = const. (independent of z' and t'), it is useful in analysing the orbit equation (13) to introduce the bounce frequency $\hat{\omega}_B(\gamma_j')$ defined by[23]

$$\hat{\omega}_B(\gamma_j') = (c^2 k_p'^2 a_w \hat{a}_s^0/\gamma_j'^2)^{\frac{1}{2}} \ . \tag{20}$$

Here, $a_w > 0$ and $\hat{a}_s^0 > 0$ are assumed without loss of generality, and $\hat{\omega}_B(\gamma_j')$ is the effective bounce frequency of deeply trapped electrons with energy γ_j'. A detailed analysis[23] of Eqs.(10) and (13) shows that the zero-order electron motion is <u>untrapped</u> for energies γ_j' satisfying (Figs. 1 and 2)

$$\gamma_j' > \hat{\gamma}_+' \equiv \left[1 + (a_w + \hat{a}_s^0)^2\right]^{\frac{1}{2}} \ . \tag{21}$$

That is, when Eq.(21) is satisfied, the particle motion is modulated by the ponderomotive potential, but the normalized velocity $d\theta_{js}^0/dt'$ does not change polarity (Fig. 1). On the other hand, for $\gamma_j' < \hat{\gamma}_+'$, the electrons are <u>trapped</u>, and the zero-order motion described by Eq.(13) is cyclic, corresponding to periodic motion in the ponderomotive potential. From Eqs.(10) and (13), it is readily shown that the minimum allowable energy of a trapped electron is[23]

$$\hat{\gamma}_-' \equiv \left[1 + (a_w - \hat{a}_s^0)^2\right]^{\frac{1}{2}} \ . \tag{22}$$

Because $\hat{a}_s^0 << a_w$ in the regimes of practical interest, we note from Eqs. (21) and (22) that the characteristic energy of a trapped electron is approximately $\hat{\gamma}' \equiv (1 + a_w^2)^{\frac{1}{2}}$.

The stability analysis in Secs. III and IV specializes to the case where there are two classes of electrons: untrapped electrons with energy $\gamma_j' = \hat{\gamma}_u' > \hat{\gamma}_+'$, and deeply trapped electrons with energy $\gamma_j' = \hat{\gamma}_T' \simeq \hat{\gamma}_-'$. For the deeply trapped electrons, the effective bounce frequency in the laboratory frame is defined by $\Omega_B = \hat{\omega}_B(\hat{\gamma}_-')/\gamma_p$, i.e.,

$$\Omega_B = (c^2 k_p'^2 a_w \hat{a}_s^0/\gamma_p^2 \hat{\gamma}_-'^2)^{\frac{1}{2}} . \tag{23}$$

Because $\hat{a}_s^0 << a_w$, we estimate $\hat{\gamma}_-' \simeq \hat{\gamma}' \equiv (1 + a_w^2)^{\frac{1}{2}}$ in Eq.(23), and make use of Eq.(19) to express $k_p' = \gamma_p(1 + v_p/c)k_0$. Equation (23) can then be expressed in the equivalent (and more familiar) form

$$\Omega_B = \left(1 + \frac{v_p}{c}\right)\left(\frac{a_w \hat{a}_s^0}{1 + a_w^2}\right)^{\frac{1}{2}} ck_0 . \tag{24}$$

Continuing with definitions, we denote the average density of the trapped electrons in the ponderomotive frame by $\hat{n}_T' = \hat{n}_T/\gamma_p$, and the average density of the untrapped electrons by $\hat{n}_u' = \hat{n}_u/\gamma_p$. It is convenient to introduce the corresponding plasma frequencies defined by

$$\hat{\omega}_{pT}^2 = \frac{4\pi \hat{n}_T' e^2}{m} = \frac{4\pi \hat{n}_T e^2}{\gamma_p m} ,$$

$$\hat{\omega}_{pu}^2 = \frac{4\pi \hat{n}_u' e^2}{m} = \frac{4\pi \hat{n}_u e^2}{\gamma_p m} . \tag{25}$$

A detailed investigation of Eqs.(5) and (6) (Secs. III and IV) shows

that the appropriate small parameters, $\varepsilon_T' << 1$ and $\varepsilon_u' << 1$, used in analysing the wave equations are defined by

$$\varepsilon_T' ck_p' = \frac{a_w \hat{\omega}_{pT}^2}{2\omega_s' \hat{\gamma}_-' \hat{a}_s^0} ,$$
$$\varepsilon_u' ck_p' = \frac{a_w \hat{\omega}_{pu}^2}{2\omega_s' \hat{\gamma}_u' \hat{a}_s^0} . \qquad (26)$$

Here, $\omega_s' = \gamma_p k_0 v_p$ is defined in Eq.(16), $\hat{\gamma}_u'$ is the energy of the untrapped electrons, and $\hat{\gamma}_-'$, $\hat{\omega}_{pT}^2$ and $\hat{\omega}_{pu}^2$ are defined in Eqs.(22) and (25). Note from Eqs.(25) and (26) that ε_T' and ε_u' are related by $\varepsilon_T' = (\hat{n}_T'/\hat{n}_u')(\hat{\gamma}_u'/\hat{\gamma}_-')\varepsilon_u'$. In Sec. III, we will find that ε_T' is related to the (slow) variation of the equilibrium wave phase δ_s^0 by $\partial\delta_s^0/\partial z' = \varepsilon_T' ck_p'$ [Eq.(41)].

Finally, for future reference, we introduce the small dimensionless parameter Γ_T^3 defined by[23,37]

$$\Gamma_T^3 = \frac{1}{4} \frac{a_w^2}{\hat{\gamma}_-'^3} \frac{\hat{\omega}_{pT}^2}{\gamma_p^2 c^2 k_0^2} \frac{(1 + v_p/c)}{v_p/c} << 1 . \qquad (27)$$

In the absence of untrapped electrons ($\hat{n}_u' = 0$), the quantity $(3)^{\frac{1}{2}}\Gamma_T ck_0/2$ can be identified with the linear gain (temporal growth rate) in the weak-pump regime ($\Omega_B/\Gamma_T ck_0 << 1$).[37] Moreover, from Eqs.(19), (23) (26) and (27), it can be shown that Γ_T and ε_T' are related by

$$\varepsilon_T' = 2\Gamma_T \left(\frac{\Gamma_T ck_0}{\Omega_B} \right)^2 . \qquad (28)$$

From Eq.(28), we note that $\varepsilon_T' << 1$ necessarily requires that the zero-order wave amplitude $\hat{a}_s^0$ be sufficiently large that $(\Omega_B/\Gamma_T ck_0)^2 >> 2\Gamma_T$ (a small parameter).

III. STABILITY ANALYSIS FOR SMALL-AMPLITUDE PERTURBATIONS

A. Assumptions and Model

We now make use of Eqs.(5), (6) and (13) with $\gamma_j' = \text{const.}$ [Eq.(14)] to investigate detailed stability properties for small-amplitude perturbations about a quasi-steady equilibrium state. The principal assumptions in the present analysis are the following:

(a) All of the trapped electrons are deeply trapped with a sharply defined energy $\gamma_j' = \hat{\gamma}_T' \simeq \hat{\gamma}_-' = [1 + (a_w - \hat{a}_s^0)^2]^{\frac{1}{2}}$. From Eq.(13), this implies that the trapped electrons are spatially localized ("bunched") near the bottom of the ponderomotive potential with $\theta_{js}' + \delta_s' \approx 2n\pi$, where $n = 0, \pm 1, \pm 2, \cdots$ is an integer. The average density of the trapped electrons in the ponderomotive frame is $\hat{n}_T' = \hat{n}_T/\gamma_p$.

(b) All of the untrapped electrons have a sharply defined energy $\gamma_j' = \hat{\gamma}_u' > \hat{\gamma}_+' = [1 + (a_w + \hat{a}_s^0)^2]^{\frac{1}{2}}$, where $\hat{\gamma}_u'$ is sufficiently large that the motion of the untrapped electrons is only weakly modulated by the ponderomotive potential. Strictly speaking, this requires that $\hat{\gamma}_u'^2 - \hat{\gamma}_+'^2$ be large in comparison with the total well depth $4a_w\hat{a}_s^0$.

(c) Consistent with (a) and (b), we assume that the perturbations are about a quasi-steady equilibrium state characterized by $\hat{a}_s^0 = \text{const.}$ (independent of z' and t') and $\partial\delta_s^0/\partial t' = 0$. However, a slow spatial variation of the equilibrium phase δ_s^0 is required [Eq.(41)].[37,71]

In the subsequent analysis, we denote the axial coordinate of the (deeply) trapped electrons with energy $\hat{\gamma}_T' \simeq \hat{\gamma}_-'$ by $\theta_T' = k_p' z_T'(t')$, and the axial coordinate of the untrapped electrons with energy $\hat{\gamma}_u'$ is denoted by $\theta_u' = k_p' z_u'(t')$. The corresponding bounce frequencies are defined by

$$\hat{\omega}_{BT} \equiv \hat{\omega}_B(\hat{\gamma}_-') = (c^2 k_p'^2 a_w \hat{a}_s^0/\hat{\gamma}_-'^2)^{\frac{1}{2}} ,$$
$$\hat{\omega}_{Bu} \equiv \hat{\omega}_B(\hat{\gamma}_u') = (c^2 k_p'^2 a_w \hat{a}_s^0/\hat{\gamma}_u'^2)^{\frac{1}{2}} , \tag{29}$$

where $\hat{a}_s^0$ = const. is the equilibrium amplitude of the primary electromagnetic wave. Note from Eq.(29) that $\hat{\omega}_{Bu} = (\hat{\gamma}_-'/\hat{\gamma}_u')\hat{\omega}_{BT} \simeq \hat{\omega}_{BT}$ because $\hat{\gamma}_u'$ typically exceeds $\hat{\gamma}_-'$ by only a small amount for $a_w \hat{a}_s^0 << 1$. Making use of Assumptions (a) - (c), it readily follows from Eqs.(5), (6) and (13) that the nonlinear wave equations and the equations of motion for the trapped and untrapped electrons can be expressed as

$$\left(\frac{\partial}{\partial t'} + \frac{c^2 k_s'}{\omega_s'}\frac{\partial}{\partial z'}\right)\hat{a}_s = \frac{a_w \hat{\omega}_{pT}^2}{2\omega_s' \hat{\gamma}_-'} \sin(\theta_T' + \delta_s') + \frac{a_w \hat{\omega}_{pu}^2}{2\omega_s' \hat{\gamma}_u'} \langle \sin(\theta_u' + \delta_s') \rangle_u , \tag{30}$$

$$\hat{a}_s\left(\frac{\partial}{\partial t'} + \frac{c^2 k_s'}{\omega_s'}\frac{\partial}{\partial z'}\right)\delta_s' = \frac{a_w \hat{\omega}_{pT}^2}{2\omega_s' \hat{\gamma}_-'} \cos(\theta_T' + \delta_s') + \frac{a_w \hat{\omega}_{pu}^2}{2\omega_s' \hat{\gamma}_u'} \langle \cos(\theta_u' + \delta_s') \rangle_u , \tag{31}$$

and

$$\frac{d^2}{dt'^2}\theta_T' + \hat{\omega}_{BT}^2 \frac{\hat{a}_s}{\hat{a}_s^0} \sin(\theta_T' + \delta_s') = 0 , \tag{32}$$

$$\frac{d^2}{dt'^2}\theta_u' + \hat{\omega}_{Bu}^2 \frac{\hat{a}_s}{\hat{a}_s^0} \sin(\theta_u' + \delta_s') = 0 . \tag{33}$$

In Eqs.(30) and (31), $\hat{\omega}_{pT}^2$ and $\hat{\omega}_{pu}^2$ are defined in Eq.(25), and the statistical average $\langle \cdots \rangle_u$ denotes an average over initial phases of the untrapped electrons, i.e.,

$$\langle \cdots \rangle_u \equiv \int_0^{2\pi} \frac{d\theta_u'(0)}{2\pi} \cdots . \tag{34}$$

In terms of the small parameters ϵ_T' and ϵ_u' defined in Eq.(26), the nonlinear wave equations (30) and (31) can be expressed in the equivalent form

$$\left(\frac{\partial}{\partial t'} + \frac{c^2 k_s'}{\omega_s'}\frac{\partial}{\partial z'}\right)\hat{a}_s = \epsilon_T' c k_p' \hat{a}_s^0 \sin(\theta_T' + \delta_s') + \epsilon_u' c k_p' \hat{a}_s^0 \langle \sin(\theta_u' + \delta_s') \rangle_u \ , \qquad (35)$$

and

$$\hat{a}_s\left(\frac{\partial}{\partial t'} + \frac{c^2 k_s'}{\omega_s'}\right)\delta_s' = \epsilon_T' c k_p' \hat{a}_s^0 \cos(\theta_T' + \delta_s') + \epsilon_u' c k_p' \hat{a}_s^0 \langle \cos(\theta_u' + \delta_s') \rangle_u \ . \qquad (36)$$

The coupled equations (32), (33), (35) and (36) constitute a closed description of the nonlinear evolution of the system within the context of Assumptions (a) - (c).

We now make use of Eqs.(32), (33), (35) and (36) to investigate detailed properties of the sideband instability (including the influence of both trapped and untrapped electrons) for small-amplitude perturbations about a primary electromagnetic wave with constant amplitude $\hat{a}_s^0$ and slowly varying phase δ_s^0. Each quantity is expressed as its equilibrium value plus a perturbation, i.e.,

$$\begin{aligned} \hat{a}_s &= \hat{a}_s^0 + \delta\hat{a}_s \ , \\ \delta_s' &= \delta_s^0 + \tilde{\delta}_s' \ , \\ \theta_T' &= \theta_T^0 + \delta\theta_T' \ , \\ \theta_u' &= \theta_u^0 + \delta\theta_u' \ . \end{aligned} \qquad (37)$$

For the deeply trapped electrons with $\theta_T' + \delta_s' \approx 2n\pi$, we take $n = 0$ without loss of generality in Eqs.(32), (35) and (36).

B. Equilibrium Model

We first consider equilibrium solutions to Eqs.(32), (33), (35) and (36) in the absence of perturbations, i.e., $\delta\hat{a}_s = 0$, $\tilde{\delta}'_s = 0$, $\delta\theta'_T = 0$ and $\delta\theta'_u = 0$. Consistent with the assumption that $\hat{\gamma}'_u$ is sufficiently large in comparison with $\hat{\gamma}'_+$, the zero-order orbit of an untrapped electron calculated from Eq.(33) can be approximated by

$$\theta_u^0 = \theta_u^0(0) + \beta'_u c k'_p t' \ . \tag{38}$$

Here, $\beta'_u c$ = const. is the average velocity of an untrapped electron in the ponderomotive frame. In Eq.(38), note that the modulation of the electron orbit by the ponderomotive potential has been neglected. Making use of Eq.(38) and the definition of the phase average in Eq.(34) it follows trivially that

$$\langle \sin(\theta_u^0 + \delta_s^0)\rangle_u = 0 = \langle \cos(\theta_u^0 + \delta_s^0)\rangle_u \ . \tag{39}$$

That is, in Eqs.(35) and (36), the untrapped electrons do not contribute to any change in the equilibrium amplitude $\hat{a}_s^0$ and phase δ_s^0. Therefore, an appropriate quasi-steady equilibrium state consistent with Eqs.(32), (35) and (36) is described by [37]

$$\begin{aligned} &\theta_T^0 + \delta_s^0 = 0 \ , \\ &\frac{\partial}{\partial t'}\hat{a}_s^0 = 0 = \frac{\partial}{\partial z'}\hat{a}_s^0 \ , \end{aligned} \tag{40}$$

and

$$\begin{aligned} &\frac{\partial}{\partial t'}\delta_s^0 = 0 \ , \\ &\frac{\partial}{\partial z'}\delta_s^0 = \varepsilon'_T c k'_p \ . \end{aligned} \tag{41}$$

Note from Eq.(41) that $\epsilon_T' << 1$ is required in the present analysis in order that the change in δ_s^0 is small over the scale length of the ponderomotive potential ($\lambda_p' = 2\pi k_p'^{-1}$). Making use of Eq.(28), the inequality $\epsilon_T' << 1$ is equivalent to $(\Omega_B/\Gamma_T c k_0)^2 >> 2\Gamma_T$, where Γ_T is the small parameter defined in Eq.(27).

To summarize, the equilibrium state is characterized by free-streaming untrapped electrons [Eq.(38)], trapped electrons with $\theta_T^0 + \delta_s^0 = 0$ [Eq.(40)], and a primary electromagnetic wave with constant amplitude $\hat{a}_s^0$ [Eq.(40)] and slowly varying phase with $\partial\delta_s^0/\partial z' = \epsilon_T' c k_p'$ [Eq.(41)].

C. Linearized Equations

We now linearize Eqs.(32), (33), (35) and (37) for small-amplitude perturbations about the equilibrium state described by Eqs.(38)-(41). In this regard, it is convenient to introduce the normalized amplitude perturbation $\delta\hat{A}_s$ defined by

$$\delta\hat{A}_s = \frac{\delta\hat{a}_s}{\hat{a}_s^0} \ . \tag{42}$$

For $\theta_T' + \delta_s' \approx 0$, it is straightforward to show that the small-amplitude perturbations $\delta\theta_T'$, $\delta\theta_u'$, $\delta\hat{A}_s$ and $\tilde{\delta}_s'$ evolve according to

$$\frac{d^2}{dt'^2}\delta\theta_T' + \hat{\omega}_{BT}^2(\delta\theta_T' + \tilde{\delta}_s') = 0 \ , \tag{43}$$

$$\frac{d^2}{dt'^2}\delta\theta_u' + \hat{\omega}_{Bu}^2\cos(\theta_u^0 + \delta_s^0)\delta\theta_u' \tag{44}$$

$$= -\hat{\omega}_{Bu}^2 \mathrm{Im}\left[(\delta\hat{A}_s + i\tilde{\delta}_s')\exp(i\theta_u^0 + i\delta_s^0)\right] \ ,$$

$$\left(\frac{\partial}{\partial t'} + \frac{c^2 k_s'}{\omega_s'}\frac{\partial}{\partial z'}\right)\delta\hat{A}_s = \epsilon_T' c k_p' (\delta\theta_T' + \tilde{\delta}_s')$$

$$+ \epsilon_u' c k_p' \langle (\delta\theta_u' + \tilde{\delta}_s')\cos(\theta_u^0 + \delta_s^0)\rangle_u \ , \tag{45}$$

$$\left(\frac{\partial}{\partial t'} + \frac{c^2 k_s'}{\omega_s'}\frac{\partial}{\partial z'}\right)\tilde{\delta}_s' + \epsilon_T' c k_p' \delta\hat{A}_s$$

$$= -\epsilon_u' c k_p' \langle (\delta\theta_u' + \tilde{\delta}_s')\sin(\theta_u^0 + \delta_s^0)\rangle_u \ . \tag{46}$$

In analysing Eqs.(43)-(46) it is useful to express

$$\delta\theta_u' = \delta\psi' \exp(i\theta_u^0 + i\delta_s^0) + \delta\psi'^* \exp(-i\theta_u^0 - i\delta_s^0) \ , \tag{47}$$

where the complex amplitude $\delta\psi' = \delta\psi_R' + i\delta\psi_I'$ is slowly varying, and $\delta\psi'^*$ denotes the complex conjugate of $\delta\psi'$. Making use of Eqs.(44) and (47) and $\theta_u^0 = \theta_u^0(0) + \beta_u' c k_p' t'$, it is straightforward to show that $\delta\psi'$ evolves according to

$$\left\{\frac{d^2}{dt'^2} + 2i\beta_u' c k_p' \frac{d}{dt'} + \left[\hat{\omega}_{Bu}^2 \cos(\theta_u^0 + \delta_s^0) - \beta_u'^2 c^2 k_p'^2\right]\right\}\delta\psi'$$

$$= -\frac{1}{2i}\hat{\omega}_{Bu}^2 (\delta\hat{A}_s + i\tilde{\delta}_s') \ . \tag{48}$$

For untrapped electron energy $\hat{\gamma}_u'$ sufficiently large in comparison with $\hat{\gamma}_+' = [1 + (a_w + \hat{a}_s^0)^2]^{\frac{1}{2}}$, it is valid to neglect $\hat{\omega}_{Bu}^2 \cos(\theta_u^0 + \delta_s^0)$ in comparison with $\beta_u'^2 c^2 k_p'^2$ in Eq.(48). Therefore, Eq.(48) can be approximated by

$$\left(\frac{d^2}{dt'^2} + 2i\beta_u' c k_p' \frac{d}{dt'} - \beta_u'^2 c^2 k_p'^2\right)(\delta\psi_R' + i\delta\psi_I') = -\frac{1}{2i}\hat{\omega}_{Bu}^2 (\delta\hat{A}_s + i\tilde{\delta}_s') \ . \tag{49}$$

In Eq.(49), $\delta\psi_R'$, $\delta\psi_I'$, $\delta\hat{A}_s$ and $\tilde{\delta}_s'$ are all real quantities, and it follows that $\delta\psi'^* = \delta\psi_R' - i\delta\psi_I'$ evolves according to

$$\left(\frac{d^2}{dt'^2} - 2i\beta_u' c k_p' \frac{d}{dt'} - \beta_u'^2 c^2 k_p'^2\right)(\delta\psi_R' - i\delta\psi_I') = \frac{1}{2i}\hat{\omega}_{Bu}^2(\delta\hat{A}_s - i\tilde{\delta}_s') \ . \quad (50)$$

Evidently, Eq.(49) [or Eq.(50)] describes the slow evolution of $\delta\psi_R'$ and $\delta\psi_I'$ in response to the amplifying wave perturbations $\delta\hat{A}_s$ and $\tilde{\delta}_s'$.

Substituting Eq.(47) into Eqs.(45) and (46), and making use of $\theta_u^0 = \theta_u^0(0) + \beta_u' c k_p' t'$ and the definition of the phase average in Eq.(34), it is straightforward to simplify the untrapped-electron contributions in the linearized wave equations. We readily obtain

$$\langle(\delta\theta_u' + \tilde{\delta}_s')\cos(\theta_u^0 + \delta_s^0)\rangle_u = \langle\delta\theta_u'\cos(\theta_u^0 + \delta_s^0)\rangle_u = \delta\psi_R' \ , \quad (51)$$

$$\langle(\delta\theta_u' + \tilde{\delta}_s')\sin(\theta_u^0 + \delta_s^0)\rangle_u = \langle\delta\theta_u'\sin(\theta_u^0 + \delta_s^0)\rangle_u = -\delta\psi_I' \ . \quad (52)$$

In Eqs.(51) and (52), the average of $\tilde{\delta}_s'$ times $\cos(\theta_u^0 + \delta_s^0)$ or $\sin(\theta_u^0 + \delta_s^0)$ vanishes because $\tilde{\delta}_s'$ is assumed to be slowly varying. Substituting Eqs.(51) and (52) into Eqs.(45) and (46), we obtain for the evolution of $\delta\hat{A}_s$ and $\tilde{\delta}_s'$

$$\left(\frac{\partial}{\partial t'} + \frac{c^2 k_s'}{\omega_s'}\frac{\partial}{\partial z'}\right)\delta\hat{A}_s = \varepsilon_T' c k_p'(\delta\theta_T' + \tilde{\delta}_s') + \varepsilon_u' c k_p' \delta\psi_R' \ , \quad (53)$$

$$\left(\frac{\partial}{\partial t'} + \frac{c^2 k_s'}{\omega_s'}\frac{\partial}{\partial z'}\right)\tilde{\delta}_s' = -\varepsilon_T' c k_p' \delta\hat{A}_s + \varepsilon_u' c k_p' \delta\psi_I' \ . \quad (54)$$

To summarize, in the present analysis the final set of coupled, linearized equations for $\delta\theta_T'$, $\delta\psi_R'$, $\delta\psi_I'$, $\delta\hat{A}_s$ and $\tilde{\delta}_s'$ is given by Eqs.(43), (49), (50), (53) and (54).

D. Dispersion Relation in Ponderomotive Frame

We now assume that the t'- and z'-dependence of the perturbations in Eqs.(43), (49), (50), (53) and (54) is proportional to

$$\exp[-i(\Delta\omega')t' + i(\Delta k')z'] \ , \tag{55}$$

where $\mathrm{Im}(\Delta\omega') > 0$ corresponds to instability (temporal growth). Consistent with neglecting beam dielectric effects in the dispersion relation (7), we also approximate $c^2k_s'/\omega_s' = c$ in Eqs.(53) and (54). The linearized equations (43), (49), (50), (53) and (54) then become

$$[(\Delta\omega')^2 - \hat{\omega}_{BT}^2](\delta\theta_T' + \tilde{\delta}_s') = (\Delta\omega')^2\tilde{\delta}_s' \ , \tag{56}$$

$$-(\Delta\omega' - \beta_u'ck_p')^2(\delta\psi_R' + i\delta\psi_I') = -\frac{1}{2i}\hat{\omega}_{Bu}^2(\delta\hat{A}_s + i\tilde{\delta}_s') \ , \tag{57}$$

$$-(\Delta\omega' + \beta_u'ck_p')^2(\delta\psi_R' - i\delta\psi_I') = \frac{1}{2i}\hat{\omega}_{Bu}^2(\delta\hat{A}_s - i\tilde{\delta}_s') \ , \tag{58}$$

$$-i(\Delta\omega' - c\Delta k')\delta\hat{A}_s = \varepsilon_T'ck_p'(\delta\theta_T' + \tilde{\delta}_s') + \varepsilon_u'ck_p'\delta\psi_R' \ , \tag{59}$$

$$-i(\Delta\omega' - c\Delta k')\tilde{\delta}_s' = -\varepsilon_T'ck_p'\delta\hat{A}_s + \varepsilon_u'ck_p'\delta\psi_I' \ . \tag{60}$$

In Eqs.(57) and (58), it is useful to introduce the untrapped-electron susceptibilities χ^+ and χ^- defined by

$$\chi^+(\Delta k',\Delta\omega') = \frac{\hat{\omega}_{Bu}^2}{(\Delta\omega' + \beta_u'ck_p')^2} + \frac{\hat{\omega}_{Bu}^2}{(\Delta\omega' - \beta_u'ck_p')^2} \ , \tag{61}$$

$$\chi^-(\Delta k',\Delta\omega') = \frac{\hat{\omega}_{Bu}^2}{(\Delta\omega' + \beta_u'ck_p')^2} - \frac{\hat{\omega}_{Bu}^2}{(\Delta\omega' - \beta_u'ck_p')^2} \ , \tag{62}$$

From Eqs.(57) and (58) we readily obtain

$$\delta\psi_R' = \frac{1}{4}\left(i\chi^-\hat{\delta A}_s + \chi^+\tilde{\delta}_s'\right) , \tag{63}$$

$$\delta\psi_I' = \frac{1}{4}\left(-\chi^+\hat{\delta A}_s + i\chi^-\tilde{\delta}_s'\right) , \tag{64}$$

which express $\delta\psi_R'$ and $\delta\psi_I'$ directly in terms of the perturbed amplitude $\hat{\delta A}_s$ and phase $\tilde{\delta}_s'$. Solving Eq.(56) for $\delta\theta_T' + \tilde{\delta}_s'$ in terms of $\tilde{\delta}_s'$, and substituting Eqs.(63) and (64) into Eqs.(59) and (60) give two coupled homogeneous equations for $\hat{\delta A}_s$ and $\tilde{\delta}_s'$. Setting the resulting two-by-two determinant equal to zero, we obtain, after some straightforward algebraic manipulation,

$$\left[(\Delta\omega' - c\Delta k') + \frac{1}{4}\varepsilon_u' ck_p' \chi^-\right]^2 = \left[\varepsilon_T' ck_p' \frac{(\Delta\omega')^2}{(\Delta\omega')^2 - \hat{\omega}_{BT}^2} + \frac{1}{4}\varepsilon_u' ck_p' \chi^+\right]\left[\varepsilon_T' ck_p' + \frac{1}{4}\varepsilon_u' ck_p' \chi^+\right] . \tag{65}$$

Equation (65) is the desired dispersion relation which relates the (complex) oscillation frequency $\Delta\omega'$ to the wavenumber $\Delta k'$ and the system parameters ε_T', ε_u', ck_p', etc. Here, ε_T', ε_u', χ^+ and χ^- are defined in Eqs.(26), (61) and (62).

Before investigating detailed stability properties (Sec. IV), we show that the dispersion relation (65) reduces to familiar results in two limiting cases: (a) no untrapped electrons ($\hat{n}_u' = 0$), and (b) no trapped electrons ($\hat{n}_T' = 0$).

No Untrapped Electrons ($\hat{n}_u' = 0$): For $\hat{n}_u' = 0$, it follows from Eq.(26) that $\varepsilon_u' = 0$, and Eq. (65) reduces to

$$(\Delta\omega' - c\Delta k')^2 = \varepsilon_T'^2 c^2 k_p'^2 \frac{(\Delta\omega')^2}{(\Delta\omega')^2 - \hat{\omega}_{BT}^2} . \tag{66}$$

Equation (66) can be expressed in the equivalent form

$$0 = 1 - \frac{\hat{\omega}_{BT}^2}{(\Delta\omega')^2} - \frac{\varepsilon_T'^2 c^2 k_p'^2}{(\Delta\omega' - c\Delta k')^2} , \tag{67}$$

which is the familiar dispersion relation[37,73] for the sideband instability assuming slowly varying equilibrium phase δ_s^0 and no untrapped electrons. The detailed stability properties predicted by Eq.(67) are investigated in Ref. 37.

No Trapped Electrons ($\hat{n}_T' = 0$): For $\hat{n}_T' = 0$, it follows from Eq.(26) that $\varepsilon_T' = 0$, and Eq.(65) can be expressed as

$$\begin{aligned} 0 = &\left[(\Delta\omega' - c\Delta k') - \frac{1}{2}\varepsilon_u' c k_p' \frac{\hat{\omega}_{Bu}^2}{(\Delta\omega' - \beta_u' c k_p')^2}\right] \\ &\times \left[(\Delta\omega' - c\Delta k') + \frac{1}{2}\varepsilon_u' c k_p' \frac{\hat{\omega}_{Bu}^2}{(\Delta\omega' + \beta_u' c k_p')^2}\right] , \end{aligned} \tag{68}$$

where ε_u' and $\hat{\omega}_{Bu}^2$ are defined in Eqs.(26) and (29), and use has been made of Eqs.(61) and (62). Apart from a sign, the two factors in Eq.(68) are identical under the (simultaneous) reflections $\Delta\omega' \to -\Delta\omega'$ and $\Delta k' \to -\Delta k'$. Setting the first factor in Eq.(68) equal to zero gives the dispersion relation

$$(\Delta\omega' - c\Delta k')(\Delta\omega' - \beta_u' c k_p')^2 = \frac{a_w^2 \hat{\omega}_{pu}^2 c^2 k_p'^2}{4\hat{\gamma}_u'^3 \omega_s'} , \tag{69}$$

where use has been made of Eqs.(26) and (29). Consistent with Assumption (b), we note that Eq.(69) is independent of the equilibrium wave amplitude $\hat{a}_s^0$.

When $\Delta\omega'$ and $\Delta k'$ are transformed back to the laboratory frame, it is straightforward to show that Eq.(69) is similar to the Compton-regime dispersion relation[66] obtained in the small-signal limit in the absence of trapped electrons.

We now return to the full dispersion relation in Eq.(65).

Alternate Form of the Full Dispersion Relation: It is useful to rewrite Eq.(65) in an alternate form which clearly delineates the trapped- and untrapped-electron contributions. Making use of Eqs.(61) and (62), rearranging terms in Eq.(65), and multiplying Eq.(65) by $[(\Delta\omega')^2 - \hat{\omega}_{BT}^2]/(\Delta\omega')^2(\Delta\omega' - c\Delta k')^2$, it is straightforward to show that the dispersion relation can be expressed in the equivalent form

$$1 - \frac{\hat{\omega}_{BT}^2}{(\Delta\omega')^2} - \frac{\varepsilon_T'^2 c^2 k_p'^2}{(\Delta\omega' - c\Delta k')^2}$$

$$= \frac{1}{2}\varepsilon_u' c k_p' \hat{\omega}_{Bu}^2 \frac{[(\Delta\omega')^2 - \hat{\omega}_{BT}^2]}{(\Delta\omega')^2(\Delta\omega' - c\Delta k')^2[(\Delta\omega')^2 - \beta_u'^2 c^2 k_p'^2]^2}$$

$$\times \left\{ \frac{1}{2}\varepsilon_u' c k_p' \hat{\omega}_{Bu}^2 + 4\Delta\omega'(\Delta\omega' - c\Delta k')\beta_u' c k_p' \right.$$

$$\left. + \varepsilon_T' c k_p' [(\Delta\omega')^2 + \beta_u'^2 c^2 k_p'^2] \left[1 + \frac{(\Delta\omega')^2}{(\Delta\omega')^2 - \hat{\omega}_{BT}^2} \right] \right\} . \tag{70}$$

Here, ε_T', ε_u', $\hat{\omega}_{BT}$ and $\hat{\omega}_{Bu}$ are defined in Eqs.(26) and (29). In the absence of untrapped electrons ($\varepsilon_u' = 0$), we note that Eq.(70) reduces directly to the familiar dispersion relation (67) for the sideband instability. That is, the effects of the untrapped electrons (the terms proportional to ε_u') are incorporated on the right-hand side of Eq.(70).

IV. ANALYSIS OF DISPERSION RELATION

A. Dispersion Relation in Laboratory Frame

We now transform the full dispersion relation (70) back to the laboratory frame. From Eq.(15), it follows that

$$\begin{aligned} \Delta\omega' &= \gamma_p(\Delta\omega - v_p\Delta k) , \\ \Delta k' &= \gamma_p[\Delta k - (v_p/c^2)\Delta\omega] , \end{aligned} \tag{71}$$

where $\Delta\omega$ and Δk are the frequency and wavenumber of the perturbations in the laboratory frame. Making use of Eq.(71) and $\gamma_p^2 = (1 - v_p^2/c^2)^{-1}$, it is straightforward to show that[37]

$$\Delta\omega' - c\Delta k' = \gamma_p(1 + v_p/c)\left[(\Delta\omega - v_p\Delta k) - ck_0 \frac{v_p}{c}\frac{\Delta k}{k_s}\right] , \tag{72}$$

where $k_s = \gamma_p^2(1 + v_p/c)(v_p/c)k_0$ is defined in Eq.(18). We further introduce the shorthand notation

$$\begin{aligned} \Delta\Omega &= \Delta\omega - v_p\Delta k , \\ \Delta K &= k_0 \frac{v_p}{c}\frac{\Delta k}{k_s} . \end{aligned} \tag{73}$$

Then, from Eqs.(71)-(73), $\Delta\omega'$ and $\Delta\omega' - c\Delta k'$ can be expressed in the equivalent form

$$\begin{aligned} \Delta\omega' &= \gamma_p\Delta\Omega , \\ \Delta\omega' - c\Delta k' &= \gamma_p(1 + v_p/c)(\Delta\Omega - c\Delta K) . \end{aligned} \tag{74}$$

Equation (74) expresses $\Delta\omega'$ and $\Delta\omega' - c\Delta k'$ directly in terms of $\Delta\Omega$ and ΔK, which are related to $\Delta\omega$ and Δk in the laboratory frame by Eq.(73).

To simplify the dispersion relation (70), it is convenient to introduce the dimensionless parameter

$$\alpha_u = \frac{\hat{n}_u'}{\hat{n}_T'}\left(\frac{\hat{\gamma}_-'}{\hat{\gamma}_u'}\right)^3 , \tag{75}$$

which is a measure of the ratio of the untrapped electron density to the trapped electron density, $\hat{n}_u'/\hat{n}_T' = \hat{n}_u/\hat{n}_T$. Making use of the definitions of $\omega_s' = \gamma_p k_0 v_p$ [Eq.(16)], $k_p' = \gamma_p(1 + v_p/c)k_0$ [Eq.(19)], $\hat{\omega}_{pT}^2$ and $\hat{\omega}_{pu}^2$ [Eq.(25)], $\hat{\epsilon}_T'$ and ϵ_u' [Eqs.(26) and (28)], $\hat{\omega}_{BT}^2$ and $\hat{\omega}_{Bu}^2$ [Eq.(29)], and α_u [Eq.(75)], some straightforward algebra shows that $\epsilon_T' ck_p'$ and $\epsilon_u' ck_p' \hat{\omega}_{Bu}^2$ can be expressed in the equivalent forms

$$\epsilon_T' ck_p' = 2\Gamma_T ck_0 \left(\frac{\Gamma_T ck_0}{\Omega_B}\right)^2 \gamma_p(1 + v_p/c) , \tag{76}$$

and

$$\epsilon_u' ck_p' \hat{\omega}_{Bu}^2 = 2\alpha_u(\Gamma_T ck_0)^3 \gamma_p^3(1 + v_p/c) . \tag{77}$$

Here, Γ_T is the (small) dimensionless gain parameter defined in Eq.(27), and the bounce frequency $\Omega_B = (c^2 k_p'^2 a_w \hat{a}_s^0/\hat{\gamma}_-'^2\gamma_p^2)^{\frac{1}{2}}$ of the deeply trapped electrons is defined in the laboratory frame in Eqs.(23) and (24). Finally, making use of $k_p' = \gamma_p(1 + v_p/c)k_0$ [Eq.(19)], we note that $\beta_u' ck_p' = \gamma_p(1 + v_p/c)\beta_u' ck_0$. It is useful to define

$$\hat{\beta}_u' = (1 + v_p/c)\beta_u' \tag{78}$$

so that $\beta_u' ck_p'$ can be expressed in the compact form

$$\beta_u' ck_p' = \gamma_p \hat{\beta}_u' ck_0 \ . \tag{79}$$

After some algebraic manipulation that makes use of $\Omega_B = \hat{\omega}_{BT}/\gamma_p$ and Eqs.(74), (76), (77) and (79), it is straightforward to show that the dispersion relation (70) can be expressed in the equivalent form

$$\begin{aligned} 1 - \frac{\Omega_B^2}{(\Delta\Omega)^2} - \frac{4\Omega_B^2(\Gamma_T ck_0/\Omega_B)^6}{(\Delta\Omega - c\Delta K)^2} \\ = \alpha_u \frac{(\Gamma_T ck_0)^3[(\Delta\Omega)^2 - \Omega_B^2]}{(\Delta\Omega)^2(\Delta\Omega - c\Delta K)^2[(\Delta\Omega)^2 - \hat{\beta}_u'^2 c^2 k_0^2]^2} \\ \times \left\{ \alpha_u(\Gamma_T ck_0)^3 + 4(\Delta\Omega)(\Delta\Omega - c\Delta K)\hat{\beta}_u' ck_0 \right. \\ \left. + 2(\Gamma_T ck_0)\left(\frac{\Gamma_T ck_0}{\Omega_B}\right)^2 [(\Delta\Omega)^2 + \hat{\beta}_u'^2 c^2 k_0^2]\left[1 + \frac{(\Delta\Omega)^2}{(\Delta\Omega)^2 - \Omega_B^2}\right]\right\} . \end{aligned} \tag{80}$$

Here, $\alpha_u = (\hat{n}_u'/\hat{n}_T')(\hat{\gamma}_-'/\hat{\gamma}_u')^3$ [Eq.(75)], $\Delta\Omega = \Delta\omega - v_p\Delta k$ [Eq.(73)], $\Delta K = k_0(v_p/c)\Delta k/k_s$ [Eq.(73)], and Γ_T is the (small) dimensionless gain parameter defined in Eq.(27). For $a_w\hat{a}_s^0 << 1$, we estimate $\hat{\gamma}_-' \simeq (1 + a_w^2)^{\frac{1}{2}}$ in Eq.(27), and Γ_T can also be expressed in the more familiar form

$$\Gamma_T^3 = \frac{1}{4} \frac{a_w^2}{(1 + a_w^2)^{3/2}} \frac{(4\pi\hat{n}_T e^2/m)}{\gamma_p^3 c^2 k_0^2} \frac{(1 + v_p/c)}{v_p/c} << 1 \ , \tag{81}$$

where use has been made of $\hat{n}_T' = \hat{n}_T/\gamma_p$. Consistent with Assumption (b) at at the beginning of Sec. III, we require that $\hat{\beta}_u' ck_0$ be sufficiently large in comparison with Ω_B in Eq.(80) in order that the untrapped-electron motion be only weakly modulated by the ponderomotive potential.

Equation (80) constitutes the final dispersion relation which is analysed numerically in Sec. IV.B. For $\alpha_u = 0$, which corresponds to no untrapped electrons ($\hat{n}_u' = 0$), Eq.(80) is the familiar dispersion relation[37,71] for the sideband instability in circumstances where the equilibrium wave phase is slowly varying [Eq.(41)]. For $\alpha_u \neq 0$, however, it is found that the untrapped electrons can significantly modify stability behavior (Sec. IV.B).

B. Numerical Results

In analysing the dispersion relation (80) it is sensible to introduce the total density of beam electrons $\hat{n}_b = \hat{n}_T + \hat{n}_u$. We define the fraction of beam electrons that are untrapped (f_u) and the fraction of beam electrons that are trapped (f_T) by

$$f_u = \frac{\hat{n}_u}{\hat{n}_b} ,$$
$$f_T = \frac{\hat{n}_T}{\hat{n}_b} = 1 - f_u . \tag{82}$$

(Keep in mind that $\hat{n}_u' = \hat{n}_u/\gamma_p$, $\hat{n}_T' = \hat{n}_T/\gamma_p$ and $\hat{n}_b' = \hat{n}_b/\gamma_p$ are the densities in the ponderomotive frame. Therefore, f_u and f_T are also given by $f_u = \hat{n}_u'/\hat{n}_b'$ and $f_T = \hat{n}_T'/\hat{n}_b'$.) We further define the gain factor Γ_b associated with the total beam density by

$$\Gamma_b^3 = \frac{\hat{n}_b}{\hat{n}_T} \Gamma_T^3 , \tag{83}$$

where Γ_T^3 is defined in Eq.(81). Because $(\hat{\gamma}_-'/\hat{\gamma}_u')^3 \simeq 1$ for $a_w \hat{a}_s^0 \ll 1$, it follows from Eq.(75) that $\alpha_u = \hat{n}_u'/\hat{n}_T' = \hat{n}_u/\hat{n}_T$ is an excellent approximation.

Therefore, from Eqs.(82) and (83), $\alpha_u \Gamma_T^3$ and Γ_T^3 can be expressed in terms of Γ_b^3 and f_u by

$$\alpha_u \Gamma_T^3 = f_u \Gamma_b^3 \ ,$$
$$\Gamma_T^3 = (1 - f_u)\Gamma_b^3 \ , \tag{84}$$

where $f_u = \hat{n}_u/\hat{n}_b$ is the fraction of beam electrons that are untrapped.

In the numerical analysis of Eq.(80), we normalize all frequencies to $\Gamma_b c k_0$ and introduce the dimensionless parameters

$$\widetilde{\Delta\Omega} = \frac{\Delta\Omega}{\Gamma_b c k_0} \ , \quad \widetilde{\Delta K} = \frac{c\Delta K}{\Gamma_b c k_0} \ ,$$
$$\widetilde{\Omega}_B = \frac{\Omega_B}{\Gamma_b c k_0} \ , \quad \widetilde{\beta}_u = \frac{\hat{\beta}_u' c k_0}{\Gamma_b c k_0} \ . \tag{85}$$

In Eq.(85), note that $\widetilde{\Omega}_B = \Omega_B/\Gamma_b c k_0$ is a dimensionless measure of the pump strength (amplitude of the primary electromagnetic wave). Substituting Eqs.(84) and (85) into Eq.(80), we find that the dispersion relation can be expressed in the equivalent form

$$1 - \frac{\widetilde{\Omega}_B^2}{(\widetilde{\Delta\Omega})^2} - \frac{4(1 - f_u)^2 \widetilde{\Omega}_B^4}{(\widetilde{\Delta\Omega} - \widetilde{\Delta K})^2}$$
$$= \frac{f_u[(\widetilde{\Delta\Omega})^2 - \widetilde{\Omega}_B^2]}{(\widetilde{\Delta\Omega})^2(\widetilde{\Delta\Omega} - \widetilde{\Delta K})^2[(\widetilde{\Delta\Omega})^2 - \widetilde{\beta}_u^2]^2} \Bigg\{ f_u \tag{86}$$
$$+ 4(\widetilde{\Delta\Omega})(\widetilde{\Delta\Omega} - \widetilde{\Delta K})\widetilde{\beta}_u + \frac{2(1 - f_u)}{\widetilde{\Omega}_B^2}[(\widetilde{\Delta\Omega})^2 + \widetilde{\beta}_u^2]\left[1 + \frac{(\widetilde{\Delta\Omega})^2}{(\widetilde{\Delta\Omega})^2 - \widetilde{\Omega}_B^2}\right]\Bigg\} \ .$$

The dispersion relation (86) has been solved numerically for the normalized growth rate $\mathrm{Im}(\Delta\tilde{\Omega}) = \mathrm{Im}(\Delta\Omega)/\Gamma_b ck_0$ and the normalized real frequency $\mathrm{Re}(\Delta\tilde{\Omega}) = \mathrm{Re}(\Delta\Omega)/\Gamma_b ck_0$ versus the normalized wavenumber $\Delta\tilde{K} = \Delta K/\Gamma_b k_0$ over a wide range of system parameters $\tilde{\Omega}_B = \Omega_B/\Gamma_b ck_0$, $f_u = \hat{n}_u/\hat{n}_b$, and $\tilde{\beta}_u = \hat{\beta}_u'/\Gamma_b$. Typical results are illustrated in Figs. 3 - 8 for a fixed value of $\tilde{\beta}_u = 3 \times 2^{1/3} = 4.3267$, and normalized pump strength ranging from $\Omega_B/\Gamma_b ck_0 = 2^{1/3} = 1.2599$ (Figs. 3 - 5), to $\Omega_B/\Gamma_b ck_0 = 0.5$ (Fig. 6), to $\Omega_B/\Gamma_b ck_0 = 0.2$ (Figs. 7 and 8).

In Fig. 3, we illustrate typical numerical results and establish the sign conventions inherent in the dispersion relation (86). In particular, for $\Omega_B/\Gamma_b ck_0 = 2^{1/3}$ and $f_u = \hat{n}_u/\hat{n}_b = 0.5$, Fig. 3 shows plots of the normalized growth rate $\mathrm{Im}(\Delta\Omega)/\Gamma_b ck_0$ and real oscillation frequency $\mathrm{Re}(\Delta\Omega)/\Gamma_b ck_0$ versus normalized wavenumber $\Delta K/\Gamma_b k_0$ obtained from Eq.(86) for the two classes of unstable solutions. The results in Figs. 3(a) and 3(b) pertain to the unstable mode driven by the <u>untrapped electrons</u>, whereas the results in Figs. 3(c) and 3(d) pertain to the unstable mode driven by the <u>trapped electrons</u>. For $f_u = \hat{n}_u/\hat{n}_b = 0.5$, of course both classes of unstable modes are affected by the other population of electrons. With regard to the symmetries inherent in Eq.(86) and evident in Fig. 3, we note that

$$\begin{aligned} \mathrm{Re}\Delta\Omega(-\Delta K) &= -\mathrm{Re}\Delta\Omega(\Delta K) \ , \\ \mathrm{Im}\Delta\Omega(-\Delta K) &= \mathrm{Im}\Delta\Omega(\Delta K) \ , \end{aligned} \tag{87}$$

are (necessarily) satisfied by both classes of unstable modes. Equation (87) assures that the Fourier transform functions for the perturbed quantities $\delta\hat{A}_s, \delta\tilde{s}, \delta\theta_T'$, etc., correspond to transforms of <u>real-valued</u> functions.

For simplicity of notation, keeping in mind the symmetries in Eq.(87) and Fig. 3, throughout the remainder of this paper we display only the stability results corresponding to the right-most growth curves in Figs. 3(a) and 3(c). That is, in Figs. 4 - 8, the stability results are presented only for the right-most lobes of the growth rate curves.

Figure 4 shows plots of the normalized growth rate $\mathrm{Im}(\Delta\Omega)/\Gamma_b ck_0$ versus $\Delta K/\Gamma_b k_0$ obtained from Eq.(86) for $\Omega_B/\Gamma_b ck_0 = 2^{1/3}$ and fraction of untrapped electrons ranging from $f_u = 0$ [Fig. 4(a)] to $f_u = 1$ [Fig. 4(e)]. For $f_u = 0$, Fig. 4(a) corresponds to the familiar growth rate curve [37,73] for the sideband instability assuming slowly varying equilibrium wave phase and that all of the electrons are deeply trapped. [Indeed, for $f_u = 0$ and $\hat{\Omega}_B = 2^{1/3}$, Eq.(68) can be solved analytically,[37] which gives a useful calibration of the numerical results.] Adding an untrapped electron component, it is evident from Figs. 4(b) - 4(e) that a new unstable mode (driven by the untrapped electrons) is introduced. The untrapped-electron mode is represented by the dotted curves in Figs. 4(b) - 4(e), whereas the sideband mode is represented by the solid curves. As expected for zero energy spread, the untrapped-electron mode in Figs. 4(b) - 4(e) has a relatively broad bandwidth in ΔK-space. Moreover, as f_u is increased (thereby decreasing the fraction of trapped electrons), the growth rate and bandwidth of the sideband instability continue to decrease as f_u is increased from $f_u = 0.2$ [Fig.4(b)], to $f_u = 0.5$ [Fig. 4(c)], to $f_u = 0.8$ [Fig. 4(d)]. Indeed, for $f_u = 1$ (no trapped electrons), the sideband instability is completely absent (as expected), and only the instability driven by the untrapped electrons is present [Fig. 4(e)].

It is evident from Figs. 4(a) - 4(e) that the properties of $\mathrm{Im}(\Delta\Omega)/\Gamma_b k_0$ versus $\Delta K/\Gamma_b k_0$ differ in detail for the two unstable modes. However, an

equally striking feature of Fig. 4 is that the characteristic maximum growth rate of the most unstable mode varies by only a small amount (less that 25%) between the case where there are no untrapped electrons [$f_u = 0$ in Fig. 4(a)] to the case where there are no trapped electrons [$f_u = 1$ in Fig. 4(e)]. This suggests that it is a serious oversight to neglect the role of an untrapped-electron component when calculating the detailed linear and nonlinear evolution of the beam electrons and the radiation field.

Figure 5 shows plots of the normalized real frequency $\mathrm{Re}(\Delta\Omega)/\Gamma_b ck_0$ versus $\Delta K/\Gamma_b k_0$ obtained from Eq.(86) for $\Omega_B/\Gamma_b ck_0 = 2^{1/3}$, and $f_u = 0$ [Fig. 5(a)], $f_u = 0.5$ [Fig. 5(b)] and $f_u = 1$ [Fig. 5(c)]. The system parameters in Figs. 5(a), 5(b) and 5(c) are identical to Figs. 4(a), 5(c) and 5(e), respectively. Moreover, $\mathrm{Re}(\Delta\Omega)$ is plotted only over the unstable range of ΔK, and the solid curves in Fig. 5 correspond to the sideband mode whereas the dotted curves correspond to the untrapped-electron mode. Evidently, $\mathrm{Re}(\Delta\Omega)$ increases monotonically with ΔK for the sideband mode [Figs. 5(a) and 5(b)]. Furthermore, the magnitude of $\mathrm{Re}(\Delta\Omega)$ is somewhat larger for the untrapped-electron mode [Figs. 5(b) and 5(c)]. Moreover, $\mathrm{Re}(\Delta\Omega)$ is approximately constant for the untrapped-electron mode for ΔK in the range $\Delta K/\Gamma_b k_0 \gtrsim 5$.

In Fig. 6, the normalized pump strength is reduced to $\Omega_B/\Gamma_b ck_0 = 0.5$. In particular, Fig. 6 shows plots of the normalized growth rate $\mathrm{Im}(\Delta\Omega)/\Gamma_b ck_0$ versus $\Delta K/\Gamma_b k_0$ obtained from Eq.(86) for $\Omega_B/\Gamma_b ck_0 = 0.5$ and fraction of untrapped electrons ranging from $f_u = 0$ [Fig. 6(a)] to $f_u = 1$ [Fig. 6(e)]. In Fig. 6, the general features of the growth rate curves for the sideband mode (solid curves) and the untrapped-electron mode (dotted curves) are qualitatively similar to Fig. 4, although the bandwidth of the sideband instability is considerably larger for the smaller value of $\Omega_B/\Gamma_b ck_0$ chosen in Fig. 6 [compare Figs. 4(a) and 6(a)]. Moreover, the maximum growth rate

of the untrapped-electron mode shifts from negative values of ΔK for $f_u \lesssim 0.5$ [Figs. 6(b) and 6(c)] to positive values of ΔK for $f_u > 0.5$ [Figs. 6(d) and 6(e)]. As in Fig. 4, it is evident from Fig. 6 that the characteristic maximum growth rate of the most unstable mode varies by only a small amount over the entire range from $f_u = 0$ [Fig. 6(a)] to $f_u = 1$ [Fig. 6(e)]. However, the detailed properties of $\mathrm{Im}(\Delta\Omega)/\Gamma_b k_0$ versus $\Delta K/\Gamma_b k_0$ differ considerably for the two modes.

Finally, in Figs. 7 and 8, the normalized pump strength is reduced further to $\Omega_B/\Gamma_b ck_0 = 0.2$. Shown are plots of $\mathrm{Im}(\Delta\Omega)/\Gamma_b ck_0$ (Fig. 7) and $\mathrm{Re}(\Delta\Omega)/\Gamma_b ck_0$(Fig. 8) versus $\Delta K/\Gamma_b k_0$ obtained from Eq.(86) for $\Omega_B/\Gamma_b ck_0 = 0.2$ and values of f_u ranging from $f_u = 0$ to $f_u = 1$. As in Figs. 4 and 6, only the sideband mode is unstable for $f_u = 0$ [Fig. 7(a)], whereas only the untrapped-electron mode is unstable for $f_u = 1$ [Fig. 7(e)]. Finally, as in Figs. 4 and 6, the characteristic maximum growth rate of the most unstable mode varies by only a small amount over the entire range of f_u considered in Fig. 7.

V. CONCLUSIONS

This paper has investigated the detailed influence of untrapped electrons on the sideband instability in a helical wiggler free electron laser. Small-amplitude peturbations are assumed about a constant-amplitude ($\hat{a}_s^0$ = const.) primary electromagnetic wave with slowly varying equilibrium phase δ_s^0 [Eqs.(40) and (41)]. A simple model is adopted in whch all of the trapped electrons are deeply trapped, and the equilibrium motion of the untrapped electrons (assumed monoenergetic) is only weakly modulated by the ponderomotive potential. The theoretical model is based on the single-particle orbit equations together with Maxwell's equations and appropriate statistical averages (Sec. II). Like our recent treatment[37] of the sideband instability (which neglects the effects of untrapped electrons), the present analysis is carried out in the ponderomotive frame, which leads to a substantial simplification in deriving the dispersion relation (70) (Sec. III). Transforming Eq.(70) back to the laboratory-frame frequency $\omega = \omega_s + \Delta\omega$ and wavenumber $k = k_s + \Delta k$, detailed properties of the sideband instability are investigated, including the effects of the untrapped electrons (Sec. IV).

The resulting dispersion relation (86) has been analysed numerically over a wide range of dimensionless pump strength $\Omega_B/\Gamma_b ck_0$ and fraction of untrapped electrons $f_u = \hat{n}_u/\hat{n}_b$. To briefly summarize, when both trapped electrons and untrapped electrons are present, there are generally two types of unstable modes, which we refer to as the sideband mode, and the untrapped-electron mode. For $f_u = 0$, only the sideband instability is present (as expected). As f_u is increased, the growth rate of the sideband instability decreases, whereas the growth rate of the untrapped-electron mode increases until only the untrapped-electron mode is unstable for $f_u = 1$ (Figs. 4, 6 and 7).

It is evident from the present analysis that the detailed growth properties are quite different for the two unstable modes. However, a very important feature of the stability results is that the characteristic maximum growth rate of the most unstable mode varies by only a small amount over the entire range of f_u from $f_u = 0$ (no untrapped electrons) to $f_u = 1$ (no trapped electrons). This suggests that it is a serious oversight to neglect the role of an untrapped-electron component when calculating the detailed linear and nonlinear evolution of the beam electrons and the radiation field.

ACKNOWLEDGMENTS

This research was supported in part by the Office of Naval Research.

VI. REFERENCES

1. N.M. Kroll and W.A. McMullin, Phys. Rev. A17, 300 (1978).
2. A. Hasegawa, Bell Syst. Tech. J. 57, 3069 (1978).
3. W.B. Colson, Phys. Lett. 59A, 187 (1976).
4. V.P. Sukhatme and P.A. Wolff, J. Appl. Phys. 44, 2331 (1973).
5. C.A. Brau, IEEE J. Quantum Electronics QE-21, 824 (1985).
6. R.W. Warren, B.E. Newmam and J.C. Goldstein, IEEE J. Quantum Electronics QE-21, 882 (1985).
7. T.J. Orzechowski, B. Anderson, W.M. Fawley, D. Prosnitz, E.T. Scharlemann, S. Yarema, D.B. Hopkins, A.C. Paul, A.M. Sessler and J.S. Wurtele, Phys. Rev. Lett. 54, 889 (1985).
8. T.J. Orzechowski, E.T. Scharlemann, B. Anderson, V.K. Neil, W.M. Fawley, D. Prosnitz, S.M. Yarema, D.B. Hopkins, A.C. Paul, A.M. Sessler and J.S. Wurtele, IEEE J. Quantum Electronics QE-21, 831 (1985).
9. M. Billardon, P. Elleaume, J.M. Ortega, C. Bazin, M. Bergher, M. Velghe, D.A.G. Deacon, and Y. Petroff, IEEE J. Quantum Electronics, QE-21, 805 (1985).
10. J. Masud, T.C. Marshall, S.P. Schlesinger, and F.G. Yee, Phys. Rev. Lett. 56, 1567 (1986).
11. J. Fajans, G. Bekefi, Y.Z. Yin and B. Lax, Phys. Rev. Lett. 53, 246 (1984).
12. R.W. Warren, B.E. Newmam, J.G. Winston, W.E. Stein, L.M. Young and C.A. Brau, IEEE J. Quantum Electronics QE-19, 391 (1983).
13. G. Bekefi, R.E. Shefer and W.W. Destler, Appl. Phys. Lett. 44, 280 (1983).
14. C.W. Roberson, J.A. Pasour, F. Mako, R.F. Lucey, Jr., and P. Sprangle, Infrared and Millimeter Waves 10, 361 (1983), and references therein.

15. A. Grossman, T.C. Marshall, and S.P. Schlesinger, Phys. Fluids 26, 337 (1983).

16. D. Prosnitz and A.M. Sessler, in Physics of Quantum Electronics (Addison-Wesley, Reading, Mass.) 9, 651 (1982).

17. R.K. Parker, R.H. Jackson, S.H. Gold, H.P. Freund, V.L. Granatstein, P.C. Efthimion, M. Herndon, and A.K. Kinkead, Phys. Rev. Lett. 48, 238 (1982).

18. S. Benson, D.A.G. Deacon, J.N. Eckstein, J.M.J. Madey, K. Robinson, T.I. Smith, and R. Taber, Phys. Rev. Lett. 48A, 235 (1982).

19. A.N. Didenko, A.R. Borisov, G.R. Fomenko, A.V. Kosevnikov, G.V. Melnikov, Yu G. Stein, and A.G. Zerlitsin, IEEE Trans. Nucl. Sci. NS-28, 3169 (1981).

20. D.B. McDermott, T.C. Marshall, S.P. Schlesinger, R.K. Parker, and V.L. Granatstein, Phys. Rev. Lett. 41, 1368 (1978).

21. D.A.G. Deacon, L.R. Elias, J.M.J. Madey, G.J. Ramian, H.A. Schwettman, and T.I. Smith, Phys. Rev. Lett. 38, 892 (1977).

22. L.R. Elias, W.M. Fairbank, J.M.J. Madey, H.A. Schwettman, and T.I. Smith, Phys. Rev. Lett. 36, 717 (1976).

23. R.C. Davidson, Phys. Fluids 29, 2689 (1986).

24. R.C. Davidson, J.S. Wurtele and R.E. Aamodt, Phys. Rev. A34, 3063 (1986).

25. B. Lane and R.C. Davidson, Phys. Rev. A27, 2008 (1983).

26. A.M. Dimos and R.C. Davidson, Phys. Fluids 28, 677 (1985).

27. R.C. Davidson and Y.Z. Yin, Phys. Fluids 28, 2524 (1985).

28. T. Taguchi, K. Mima, and T. Mochizuki, Phys. Rev. Lett. 46, 824 (1981).

29. F.A. Hopf, P Meystre, M.O. Scully, and W.H. Louisell, Phys. Rev. Lett. 37, 1342 (1976).

30. R.C. Davidson and W.A. McMullin, Phys. Rev. A26, 410 (1982).

31. N.S. Ginzburg and M.A. Shapiro, Opt. Comm. 40, 215 (1982).

32. J.C. Goldstein and W.B. Colson, in Proc. International Conference on Lasers (STS Press, McLean, VA, 1982), p. 218.

33. W.B. Colson, IEEE J. Quantum Electronics QE-17, 1417 (1981).

34. P. Sprangle, C.M. Tang, and W.M. Manheimer, Phys. Rev. A21, 302 (1980).

35. W.H. Louisell, J.F. Lam, D.A. Copeland, and W.B. Colson, Phys. Rev. A19, 288 (1979).

36. N.M. Kroll, P.L. Morton and M.N. Rosenbluth, IEEE J. Quantum Electronics QE-17, 1436 (1981).

37. R.C. Davidson and J.S. Wurtele, "Single-Particle Analysis of the Free Electron Laser Sideband Instability for Primary Electromagnetic Wave with Constant Phase and Slowly Varying Phase," submitted to Physics of Fluids (1986).

38. D.C. Quimby, J.M. Slater and J.P. Wilcoxon, IEEE J. Quantum Electronics QE-21, 979 (1985).

39. N.S. Ginzburg and M.I. Petelin, Int. J. Electronics 59, 291 (1985).

40. C.M. Tang and P. Sprangle, in Free Electron Generators of Coherent Radiation (C.A. Brau, S.F. Jacobs and M.O. Scully, eds.) Proc. SPIE 453, 11 (1983).

41. R.A. Freedman and W.B. Colson, Opt. Comm. 52, 409 (1985).

42. W.B. Colson, in Proc. Seventh Int. Conf. on Free Electron Lasers, Nucl. Inst. and Meth. in Phys. Research A250, in press (1986).

43. M.N. Rosenbluth, H.V. Wong and B.N. Moore, in Free Electron Generators of Coherent Radiation (C.A. Brau, S.F. Jacobs and M.O. Scully, eds.) Proc. SPIE 453, 25 (1983).

44. A.T. Lin, Physics of Quantum Electronics 9, 867 (1982).

45. H. Al-Abawi, J.K. McIver, G.T. Moore and M.O. Scully, Physics of Quantum Electronics 8, 415 (1982).

46. W.B. Colson, Physics of Quantum Electronics 8, 457 (1982).

47. J. Goldstein, in Free Electron Generators of Coherent Radiation (C.A. Brau, S.F. Jacobs and M.O. Scully, eds.) Proc. SPIE 453, 2 (1983).

48. R.C. Davidson and Y.Z. Yin, Phys. Rev. A30, 3078 (1984).

49. G.L. Johnston and R.C. Davidson, J. Appl. Phys. 55, 1285 (1984).

50. H.P. Freund and A.K. Ganguly, Phys. Rev. A28, 3438 (1983).

51. H.S. Uhm and R.C. Davidson, Phys. Fluids 26, 288 (1983).

52. R.C. Davidson and H.S. Uhm, J. Appl. Phys. 53, 2910 (1982).

53. H.S. Uhm and R.C. Davidson, Phys. Fluids 24, 2348 (1981).

54. R.C. Davidson, W.A. McMullin and K. Tsang, Phys. Fluids 27, 233 (1983).

55. R.C. Davidson and W.A. McMullin, Phys. Fluids 26, 840 (1983).

56. W.A. McMullin and G. Bekefi, Phys. Rev. A25, 1826 (1982).

57. R.C. Davidson and W.A. McMullin, Phys. Rev. A26, 1997 (1982).

58. W.A. McMullin and G. Bekefi, Appl. Phys. Lett. 39, 845 (1981).

59. R.C. Davidson, Phys. Fluids 29, 267 (1986).

60. R.C. Davidson and J.S. Wurtele, IEEE Trans. Plasma Science PS-13, 464 (1985).

61. H.P. Freund, R.A. Kehs and V.L. Granatstein, IEEE J. Quantum Electronics QE-21, 1080 (1985).

62. H.P. Freund and A.K. Ganguly, IEEE J. Quantum Electronics QE-21, 1073 (1985).

63. B. Hafizi and R.E. Aamodt, Phys. Rev. A29, 2656 (1984).

64. P. Sprangle, C.M. Tang and I. Bernstein, Phys. Rev. A28, 2300 (1983).

65. H.P. Freund and P. Sprangle, Phys. Rev. A28, 1835 (1983).

66. R.C. Davidson and H.S. Uhm, Phys. Fluids 23, 2076 (1980).

67. P. Sprangle and R.A. Smith, Phys. Rev. A21, 293 (1980).

68. I.B. Bernstein and J.L. Hirshfield, Physica (Utrecht) 20A, 1661 (1979).

69. T. Kwan and J.M. Dawson, Phys. Fluids 22, 1089 (1979).

70. T. Kwan, J.M. Dawson and A.T. Lin, Phys. Fluids 20, 581 (1977).

71. A. Bambini and A. Renieri, Lett. Nuovo Cimento 21, 399 (1978).

72. S.T. Stenholm and A. Bambini, IEEE J. Quantum Electronics QE-17, 1363 (1981).

73. M.N. Rosenbluth, private communication (1986).

FIGURE CAPTIONS

Fig. 1. In the ponderomotive frame, electron motion in the phase space (z',p'_z) occurs on surfaces with γ' = const.

Fig. 2. Plot of the equilibrium ponderomotive potential $W(z') = \{\hat{\gamma}'^2_- + 4a_w\hat{a}_s^0\sin^2[(1/2)(k'_pz' + \delta_s^0)]\}^{\frac{1}{2}}$ versus k'_pz'. $W(z')$ is the envelope of turning points with $p'_{zj} = 0$ and $(\hat{a}_s,\delta'_s) = (\hat{a}_s^0,\delta_s^0)$ in Eq.(10). Deeply trapped electrons have energy $\gamma'_j \simeq \hat{\gamma}'_- = [1 + (a_w - \hat{a}_s^0)^2]^{\frac{1}{2}}$ [Eq.(22)]. Untrapped electrons have energy $\gamma'_j = \hat{\gamma}'_u > \hat{\gamma}'_+ = [1 + (a_w + \hat{a}_s^0)^2]^{\frac{1}{2}}$ [Eq.(21)]. Note that $\hat{\gamma}'^2_+ - \hat{\gamma}'^2_- = 4a_w\hat{a}_s^0 << 1$.

Fig. 3. Plots of the normalized growth rate $\mathrm{Im}(\Delta\Omega)/\Gamma_b ck_0$ and real frequency $\mathrm{Re}(\Delta\Omega)/\Gamma_b ck_0$ versus $\Delta K/\Gamma_b k_0$ obtained from Eq.(86) for the untrapped-electron mode [Figs. 3(a) and 3(b)] and the trapped-electron mode [Figs. 3(c) and 3(d)]. Results are presented for $\Omega_B/\Gamma_b ck_0 = 2^{1/3}$, $\tilde{\beta}_u = 3 \times 2^{1/3}$, and $f_u = 0.5$.

Fig. 4. Plots of the normalized growth rate $\mathrm{Im}(\Delta\Omega)/\Gamma_b ck_0$ versus $\Delta K/\Gamma_b k_0$ obtained from Eq.(86) for $\Omega_B/\Gamma_b ck_0 = 2^{1/3}$, $\tilde{\beta}_u = 3 \times 2^{1/3}$, and (a) $f_u = 0$, (b) $f_u = 0.2$, (c) $f_u = 0.5$, (d) $f_u = 0.8$, and (e) $f_u = 1$.

Fig. 5. Plots of the normalized real frequency $\mathrm{Re}(\Delta\Omega)/\Gamma_b ck_0$ versus $\Delta K/\Gamma_b k_0$ obtained from Eq.(86) for $\Omega_B/\Gamma_b ck_0 = 2^{1/3}$, $\tilde{\beta}_u = 3 \times 2^{1/3}$, and (a) $f_u = 0$, (b) $f_u = 0.5$, and (c) $f_u = 1$.

Fig. 6. Plots of $\mathrm{Im}(\Delta\Omega)/\Gamma_b ck_0$ versus $\Delta K/\Gamma_b k_0$ obtained from Eq.(86) for $\Omega_B/\Gamma_b ck_0 = 0.5$, $\tilde{\beta}_u = 3 \times 2^{1/3}$, and (a) $f_u = 0$, (b) $f_u = 0.2$, (c) $f_u = 0.5$, (d) $f_u = 0.8$, and (e) $f_u = 1$.

Fig. 7. Plots of $\mathrm{Im}(\Delta\Omega)/\Gamma_b ck_0$ versus $\Delta K/\Gamma_b k_0$ obtained from Eq.(86) for $\Omega_B/\Gamma_b ck_0 = 0.2$, $\tilde{\beta}_u = 3 \times 2^{1/3}$, and (a) $f_u = 0$, (b) $f_u = 0.2$, (c) $f_u = 0.5$, (d) $f_u = 0.8$, and (e) $f_u = 1$.

Fig. 8. Plots of $\mathrm{Re}(\Delta\Omega)/\Gamma_b ck_0$ versus $\Delta K/\Gamma_b k_0$ obtained from Eq.(86) for $\Omega_B/\Gamma_b ck_0 = 0.2$, $\tilde{\beta}_u = 3 \times 2^{1/3}$, and (a) $f_u = 0$, (b) $f_u = 0.5$, and (c) $f_u = 1$.

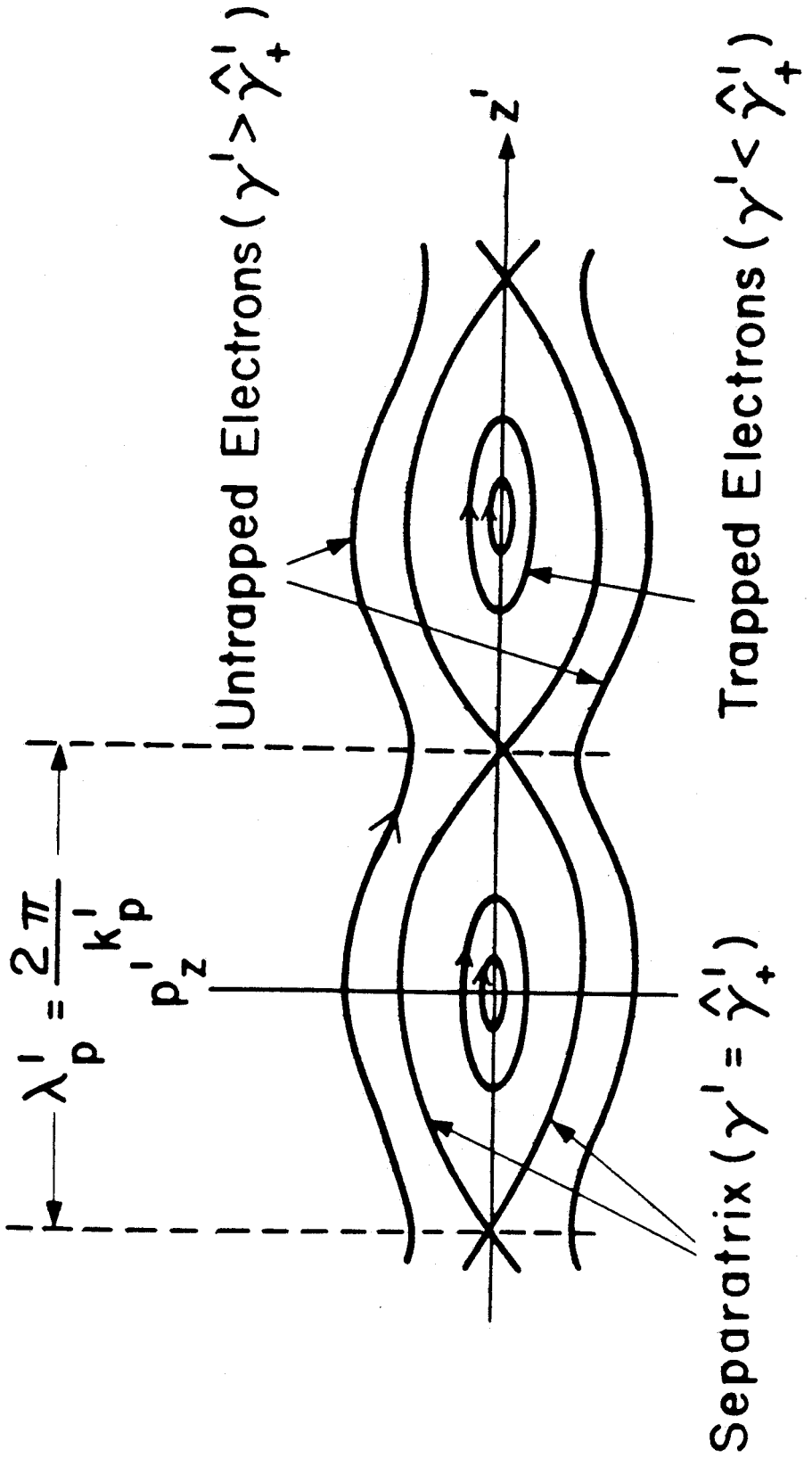
Untrapped Electrons ($\gamma' > \hat{\gamma}'_+$)
Trapped Electrons ($\gamma' < \hat{\gamma}'_+$)
Separatrix ($\gamma' = \hat{\gamma}'_+$)
z'
p'_z
$\lambda'_p = \frac{2\pi}{k'_p}$

Fig. 1

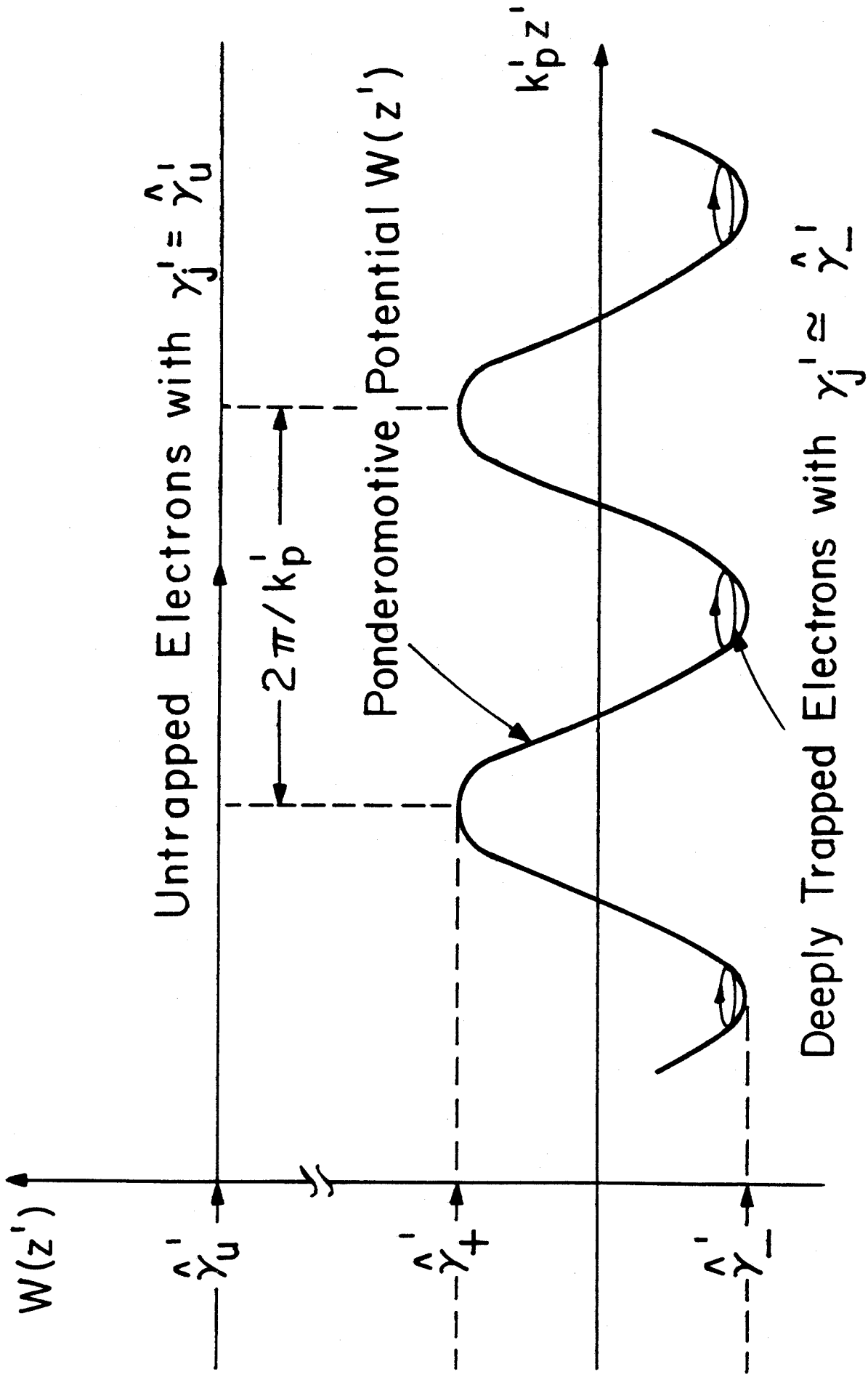
W(z')
$\hat{\gamma}'_u$
$\hat{\gamma}'_+$
$\hat{\gamma}'_-$
Untrapped Electrons with $\gamma'_j = \hat{\gamma}'_u$
$2\pi/k'_p$
Ponderomotive Potential W(z')
$k'_p z'$
Deeply Trapped Electrons with $\gamma'_j \cong \hat{\gamma}'_-$

Fig. 2

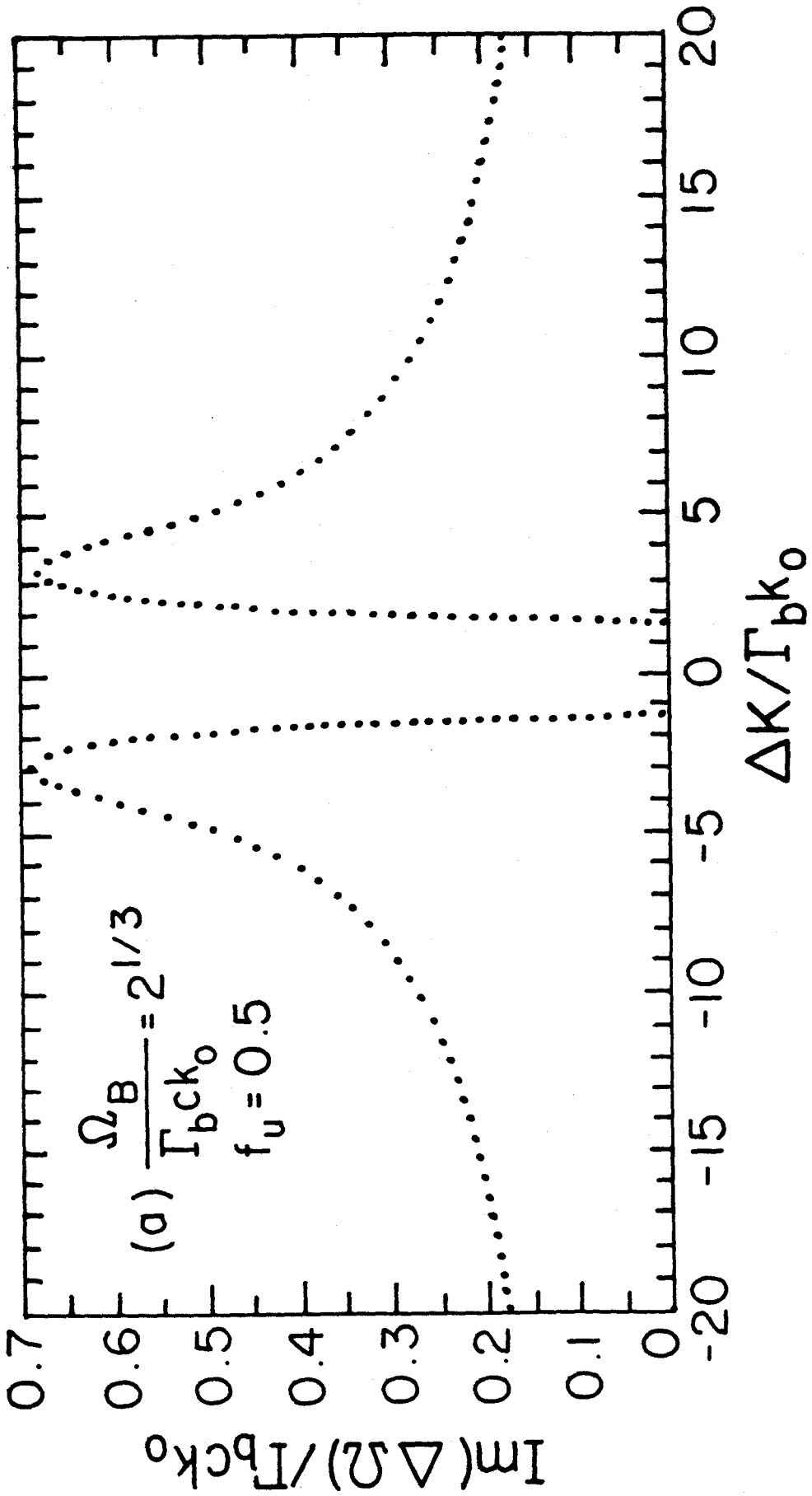
Im(ΔΩ)/Γbck0
0.7
0.6
0.5
0.4
0.3
0.2
0.1
0
-20
-15
-10
-5
0
5
10
15
20
ΔK/Γbk0
(a) ΩB/Γbck0 = 2^1/3
fu=0.5

Fig. 3(a)

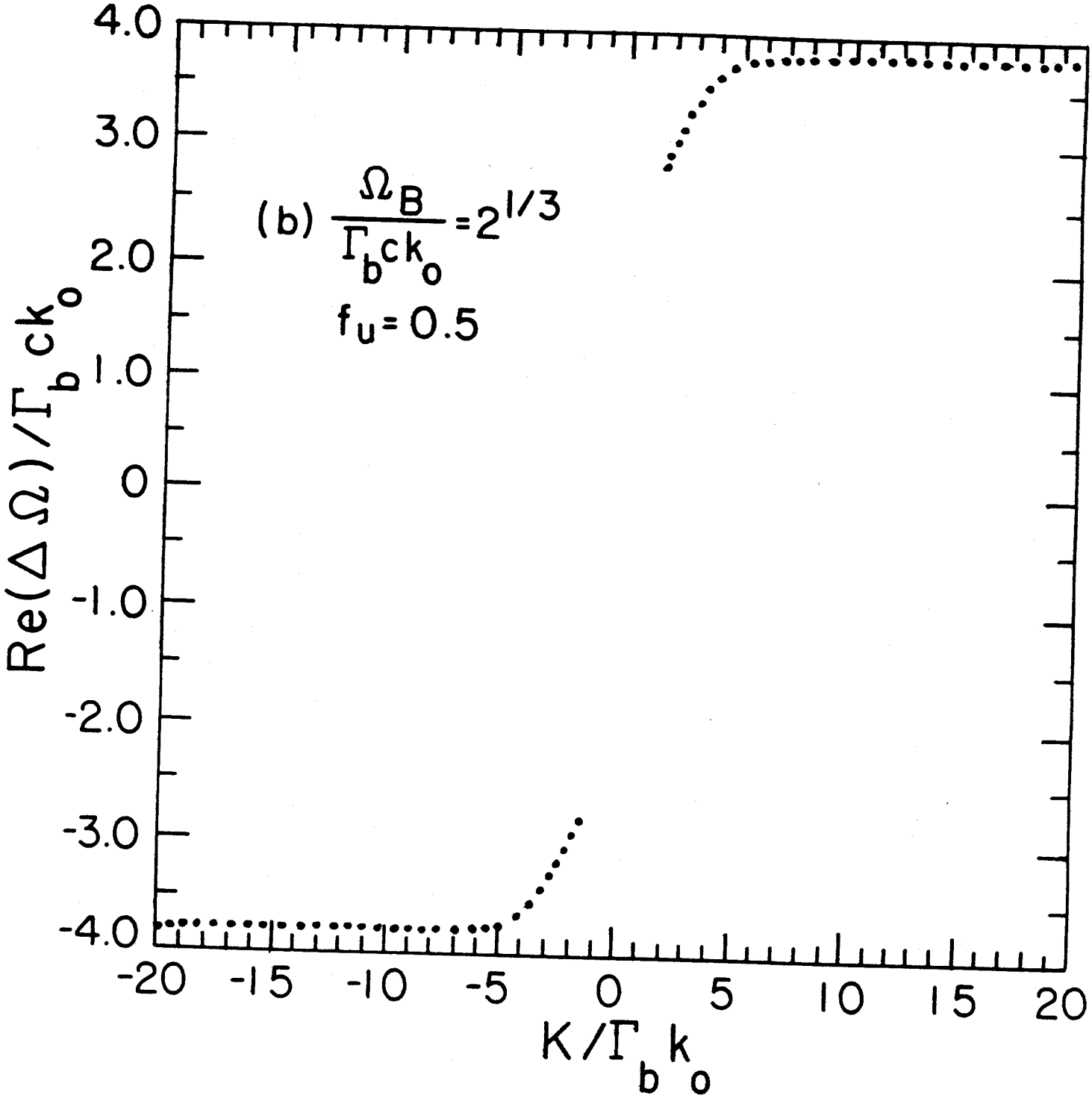
4.0
3.0
2.0
1.0
0
-1.0
-2.0
-3.0
-4.0
-20
-15
-10
-5
0
5
10
15
20
(b) $\frac{\Omega_B}{\Gamma_b c k_o} = 2^{1/3}$
$f_u = 0.5$
$\mathrm{Re}(\Delta\Omega)/\Gamma_b c k_o$
$K/\Gamma_b k_o$

Fig. 3(b)

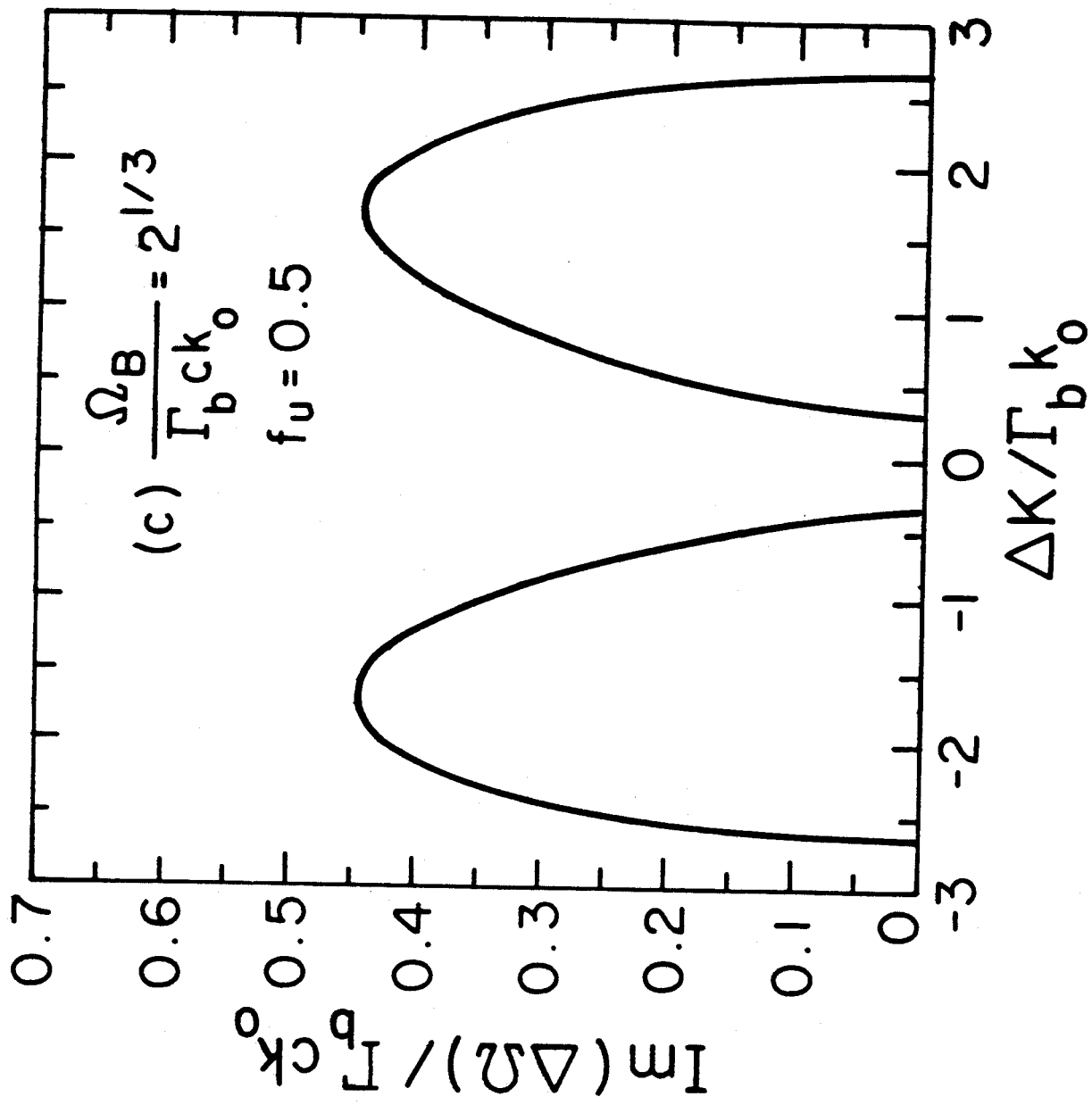
(c) $\frac{\Omega_B}{\Gamma_b c k_o} = 2^{1/3}$
$f_u = 0.5$
$\mathrm{Im}(\Delta\Omega)/\Gamma_b c k_o$
$\Delta K/\Gamma_b k_o$
0.7
0.6
0.5
0.4
0.3
0.2
0.1
0
-3
-2
-1
0
1
2
3

Fig. 3(c)

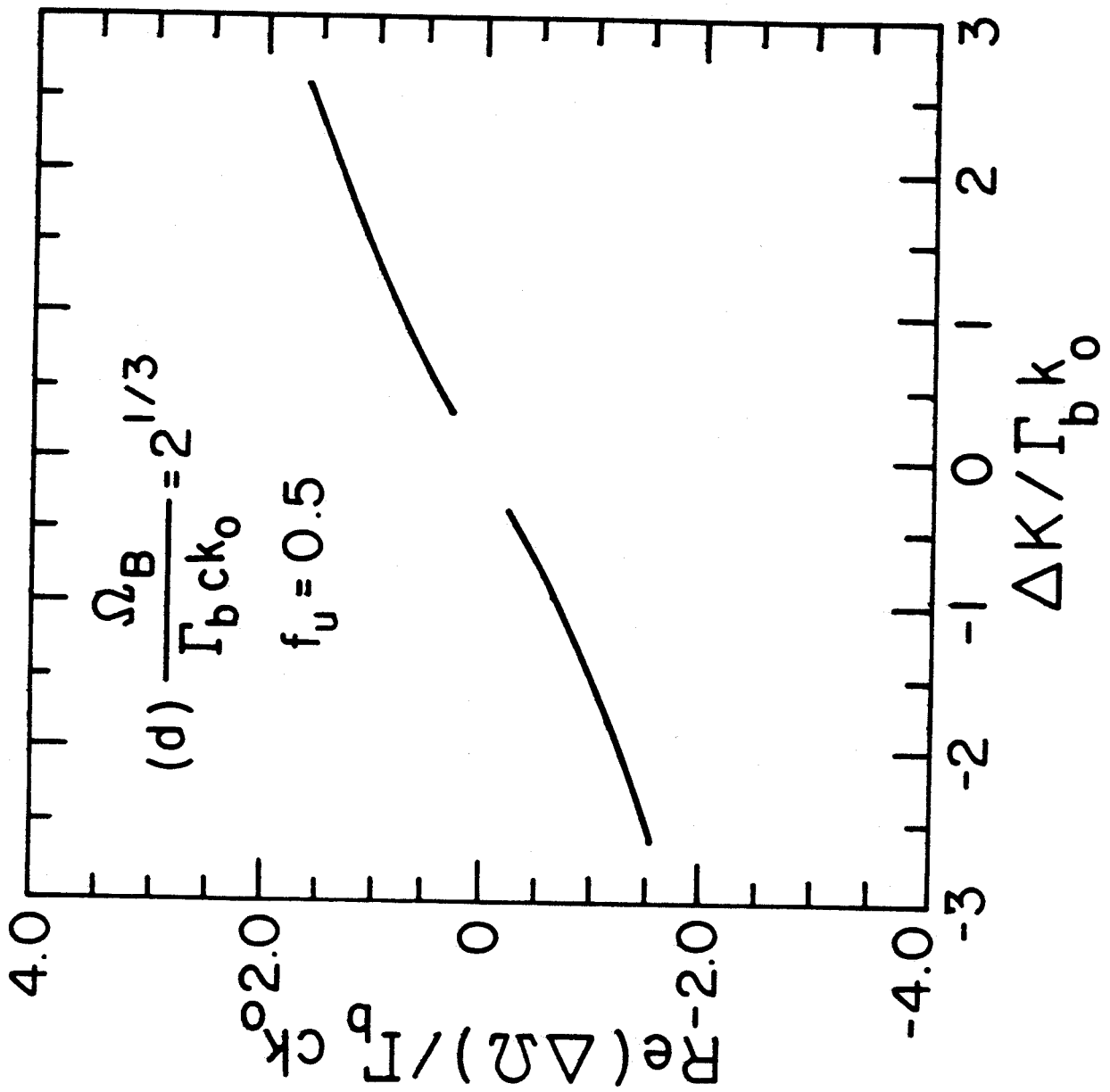
(d) $\frac{\Omega_B}{\Gamma_b c k_o} = 2^{1/3}$
$f_u = 0.5$
$\mathrm{Re}(\Delta\Omega)/\Gamma_b ck_o$
$\Delta K/\Gamma_b k_o$
4.0
2.0
0
-2.0
-4.0
-3
-2
-1
0
1
2
3

Fig. 3(d)

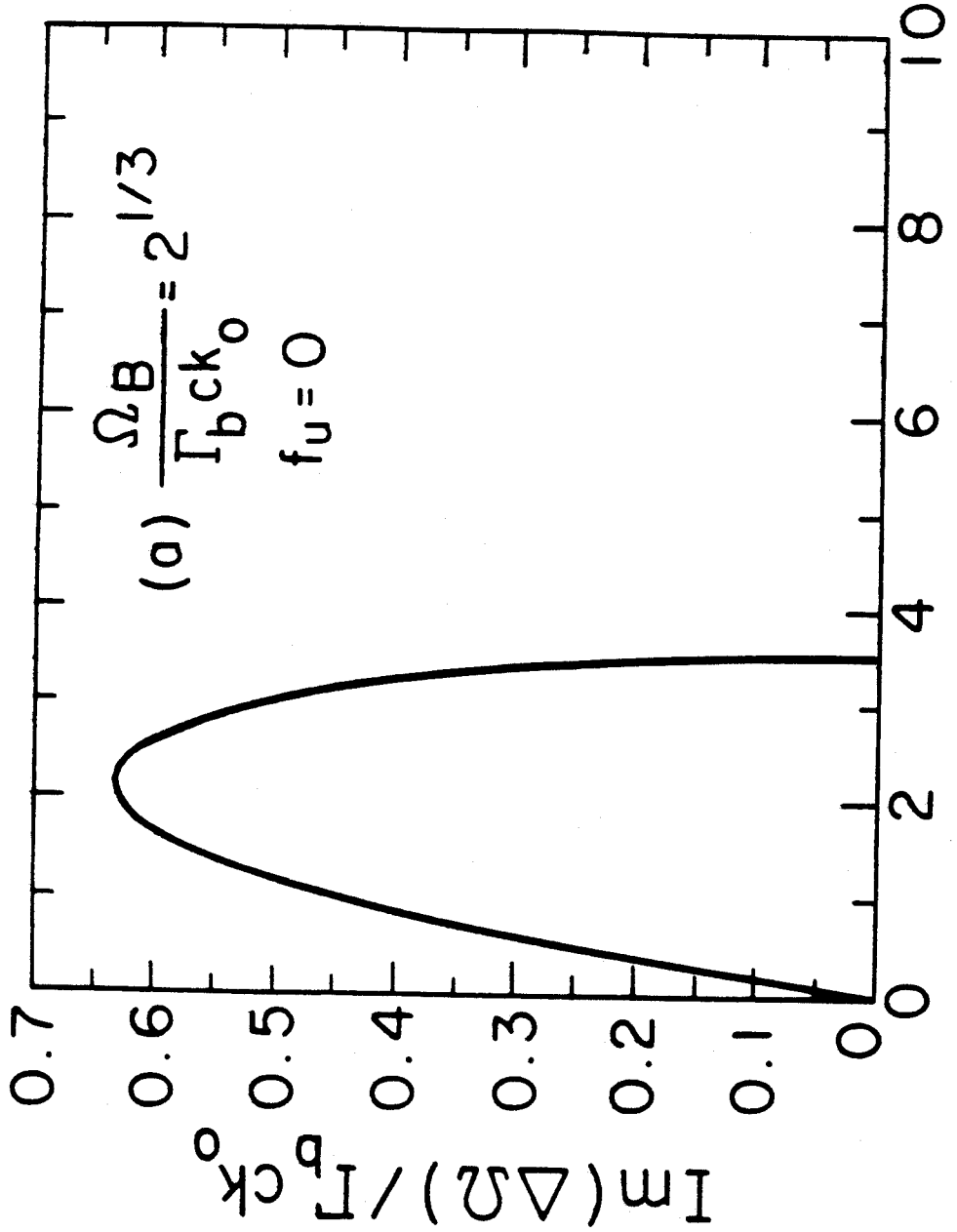
(a) $\frac{\Omega_B}{\Gamma_b c k_o} = 2^{1/3}$
$f_u = 0$
$\mathrm{Im}(\Delta\Omega)/\Gamma_b c k_o$
$\Delta K/\Gamma_b k_o$
0.7
0.6
0.5
0.4
0.3
0.2
0.1
0
2
4
6
8
10

Fig. 4(a)

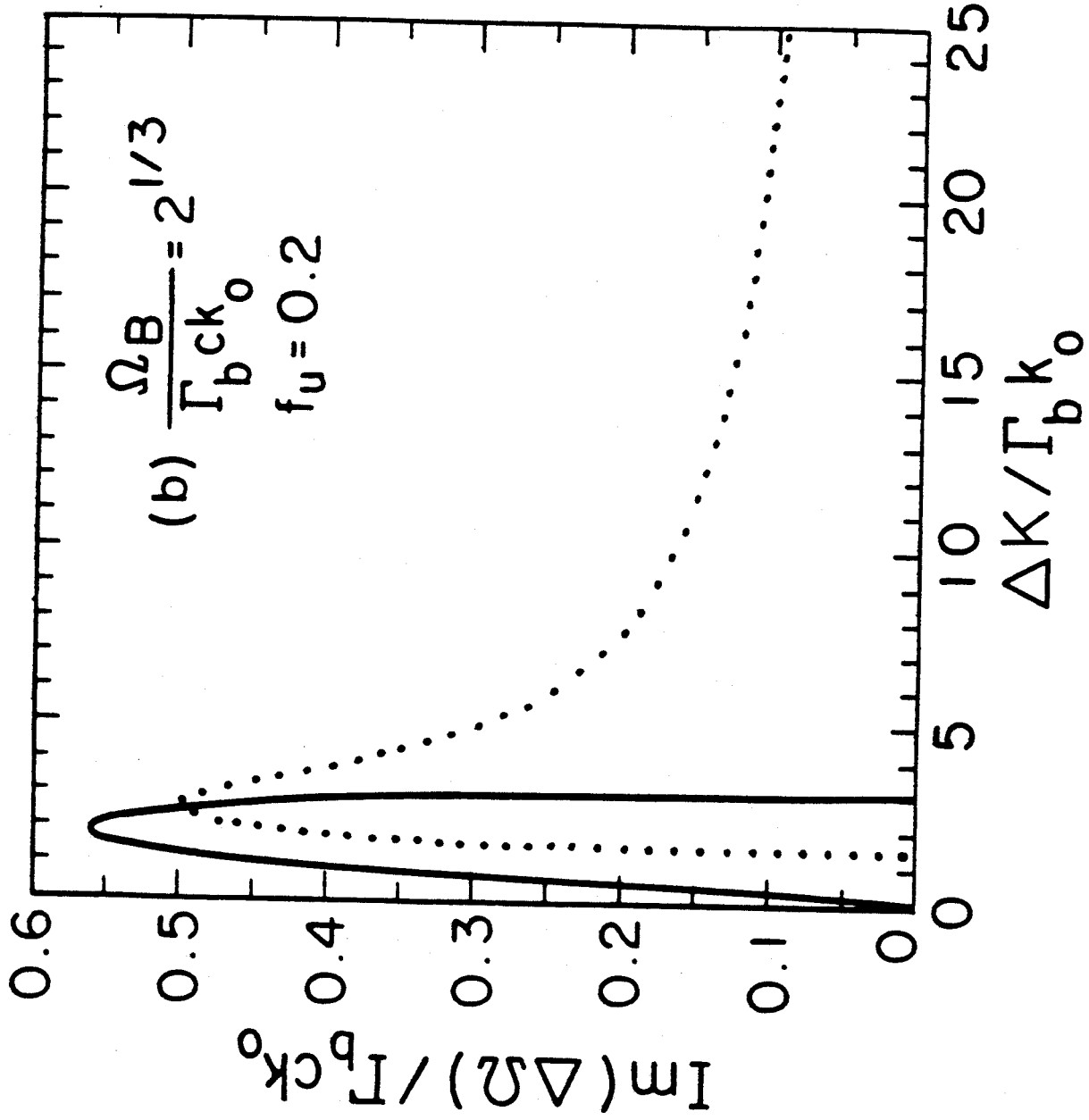
(b) $\frac{\Omega_B}{\Gamma_b c k_o} = 2^{1/3}$
$f_u = 0.2$
$\mathrm{Im}(\Delta\Omega)/\Gamma_b c k_o$
$\Delta K/\Gamma_b k_o$
0
0.1
0.2
0.3
0.4
0.5
0.6
5
10
15
20
25

Fig. 4(b)

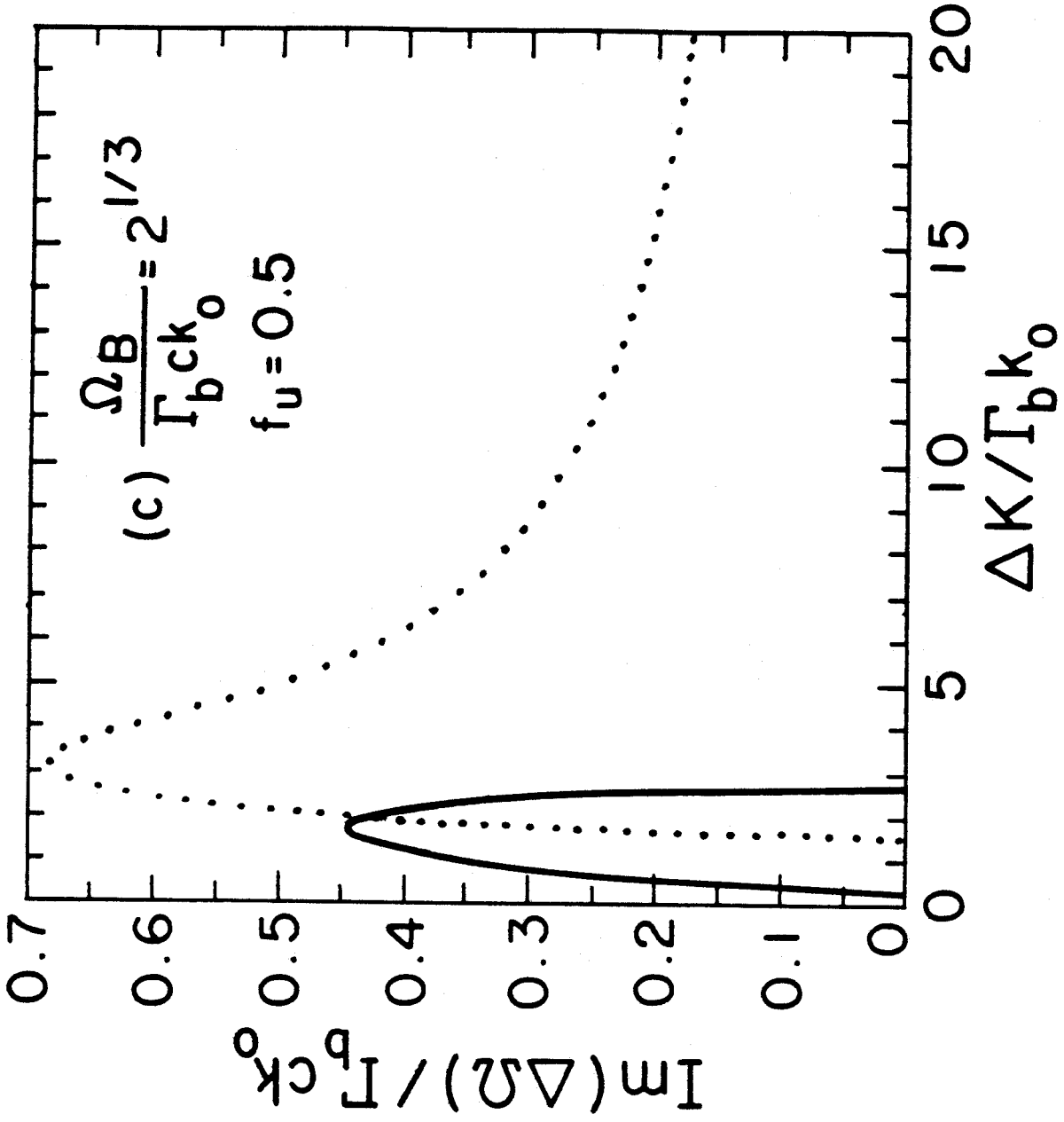
(c) $\frac{\Omega_B}{\Gamma_b c k_o} = 2^{1/3}$
$f_u = 0.5$
$\mathrm{Im}(\Delta\Omega)/\Gamma_b c k_o$
$\Delta K/\Gamma_b k_o$
0
0.1
0.2
0.3
0.4
0.5
0.6
0.7
5
10
15
20

Fig. 4(c)

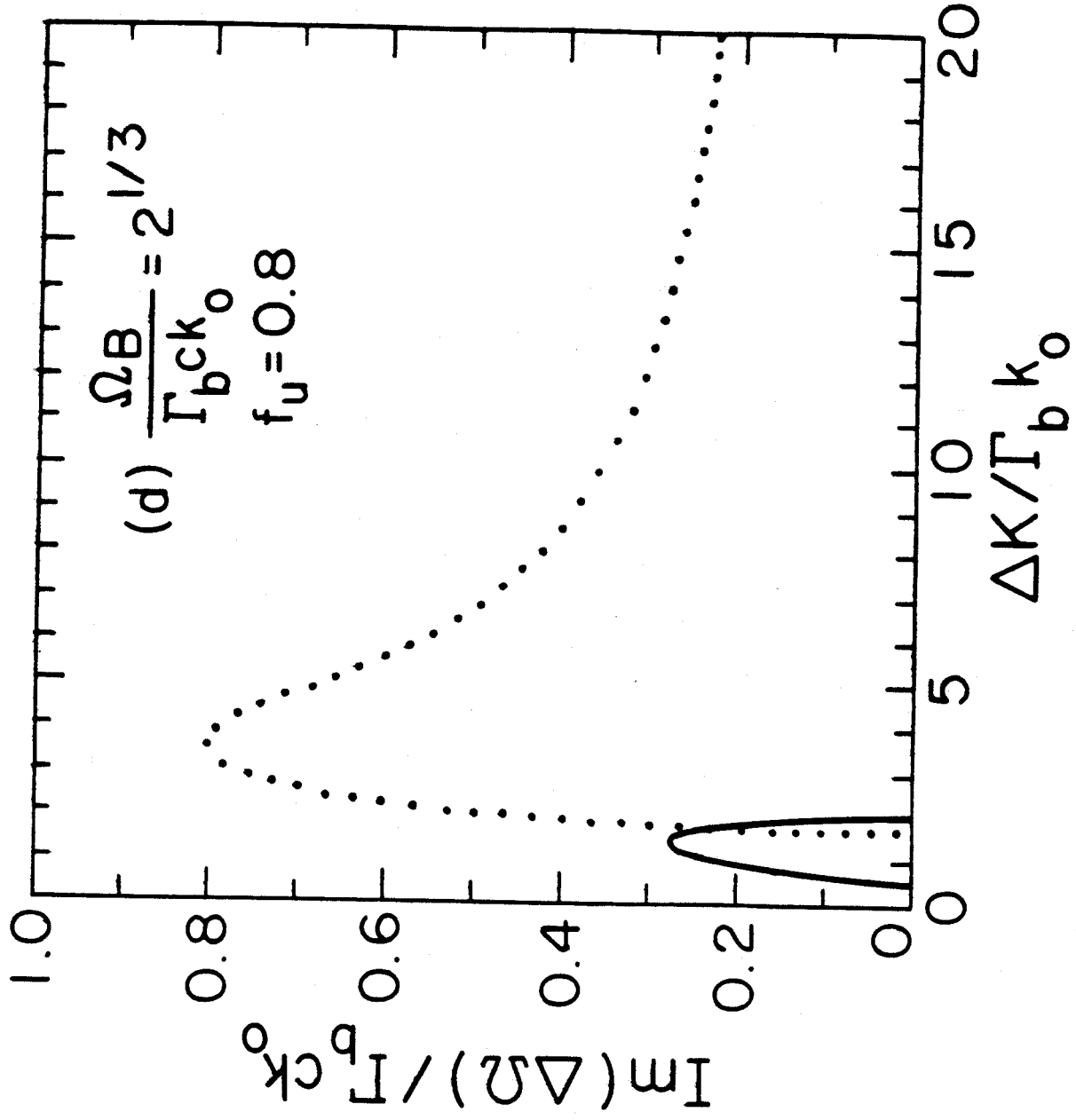
(d) $\frac{\Omega_B}{\Gamma_b c k_o} = 2^{1/3}$
$f_u = 0.8$
$\mathrm{Im}(\Delta\Omega)/\Gamma_b c k_o$
$\Delta K/\Gamma_b k_o$
0
0.2
0.4
0.6
0.8
1.0
5
10
15
20

Fig. 4(d)

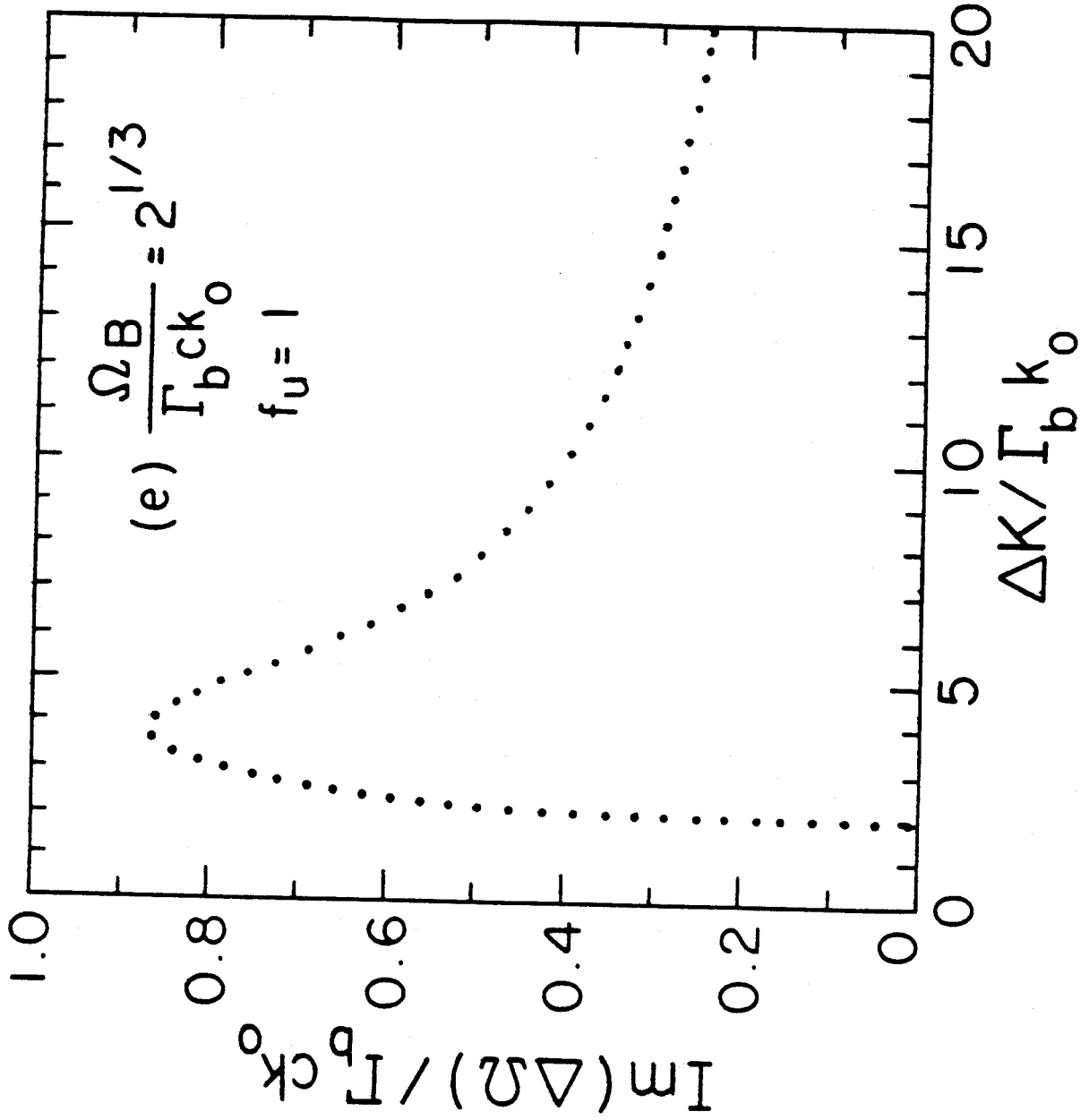
(e) $\frac{\Omega_B}{\Gamma_b c k_o} = 2^{1/3}$
$f_u = 1$
$\mathrm{Im}(\Delta\Omega)/\Gamma_b c k_o$
$\Delta K/\Gamma_b k_o$
0
0.2
0.4
0.6
0.8
1.0
5
10
15
20

Fig. 4(e)

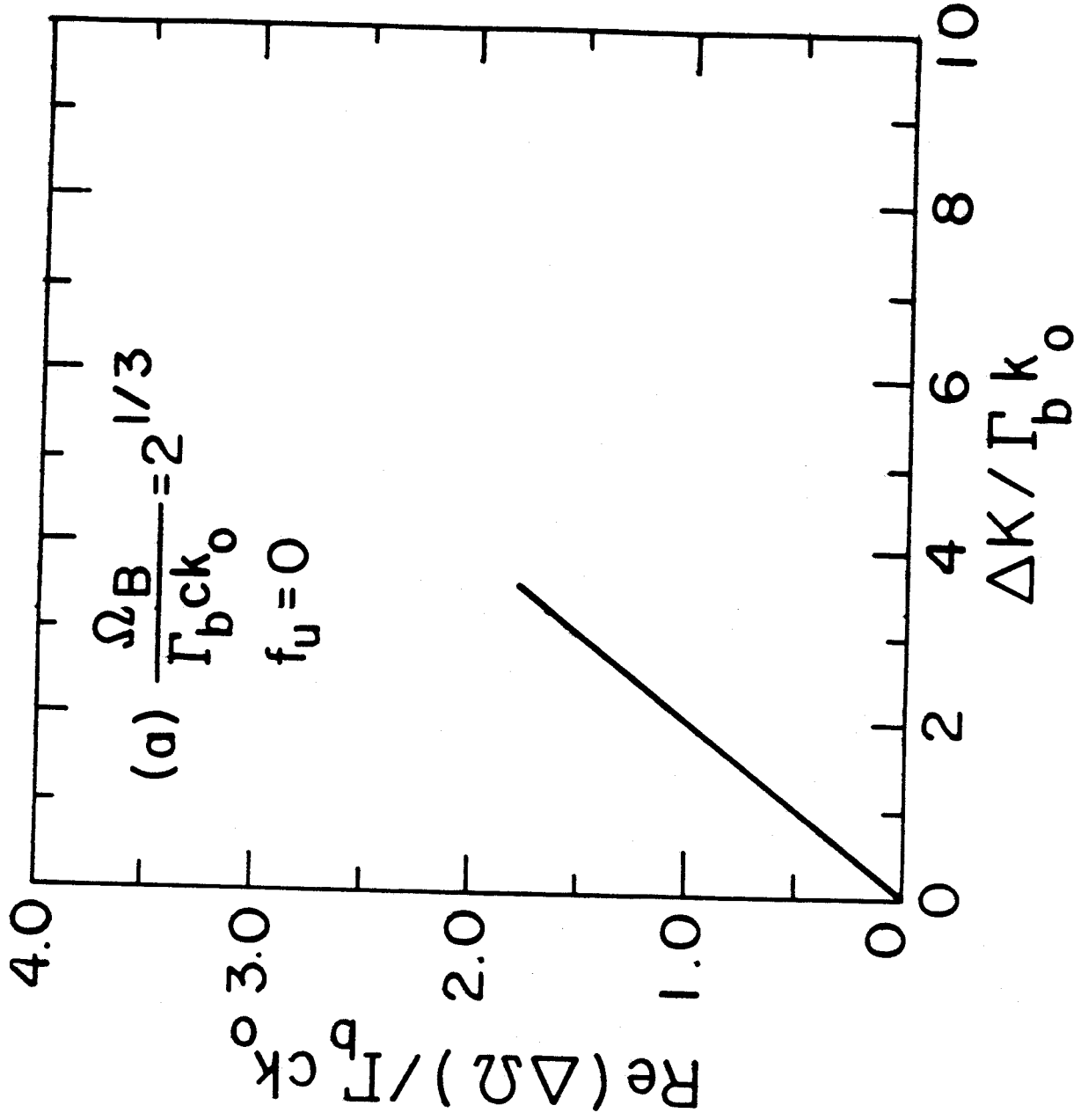
(a) $\frac{\Omega_B}{\Gamma_b c k_o} = 2^{1/3}$
$f_u = 0$
$\mathrm{Re}(\Delta\Omega)/\Gamma_b c k_o$
$\Delta K / \Gamma_b k_o$
0
1.0
2.0
3.0
4.0
2
4
6
8
10

Fig. 5(a)

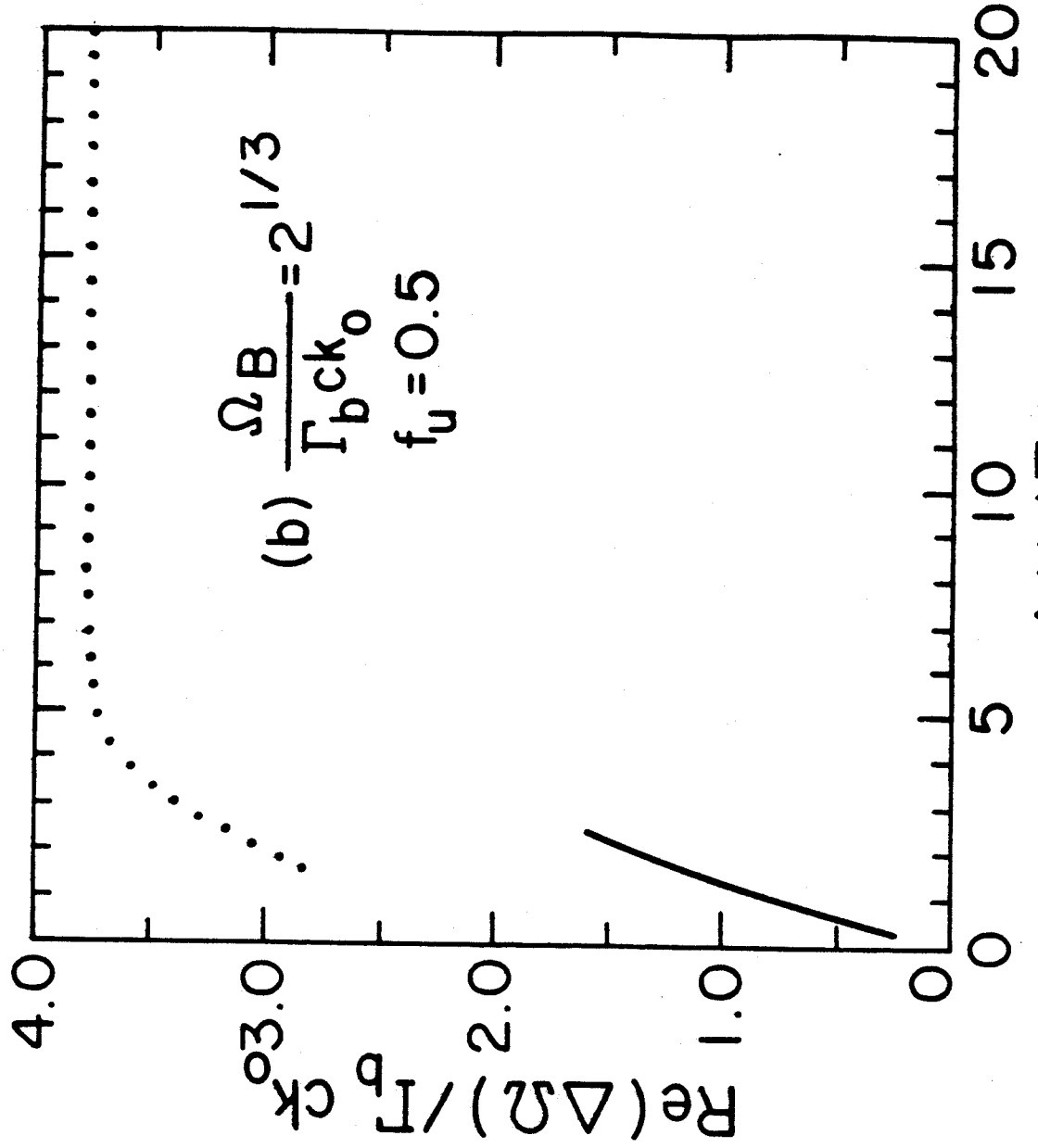
(b) $\frac{\Omega_B}{\Gamma_b c k_o} = 2^{1/3}$
$f_u = 0.5$
$\mathrm{Re}(\Delta\Omega)/\Gamma_b ck_o$
$\Delta K/\Gamma_b k_o$
0
1.0
2.0
3.0
4.0
5
10
15
20

Fig. 5(b)

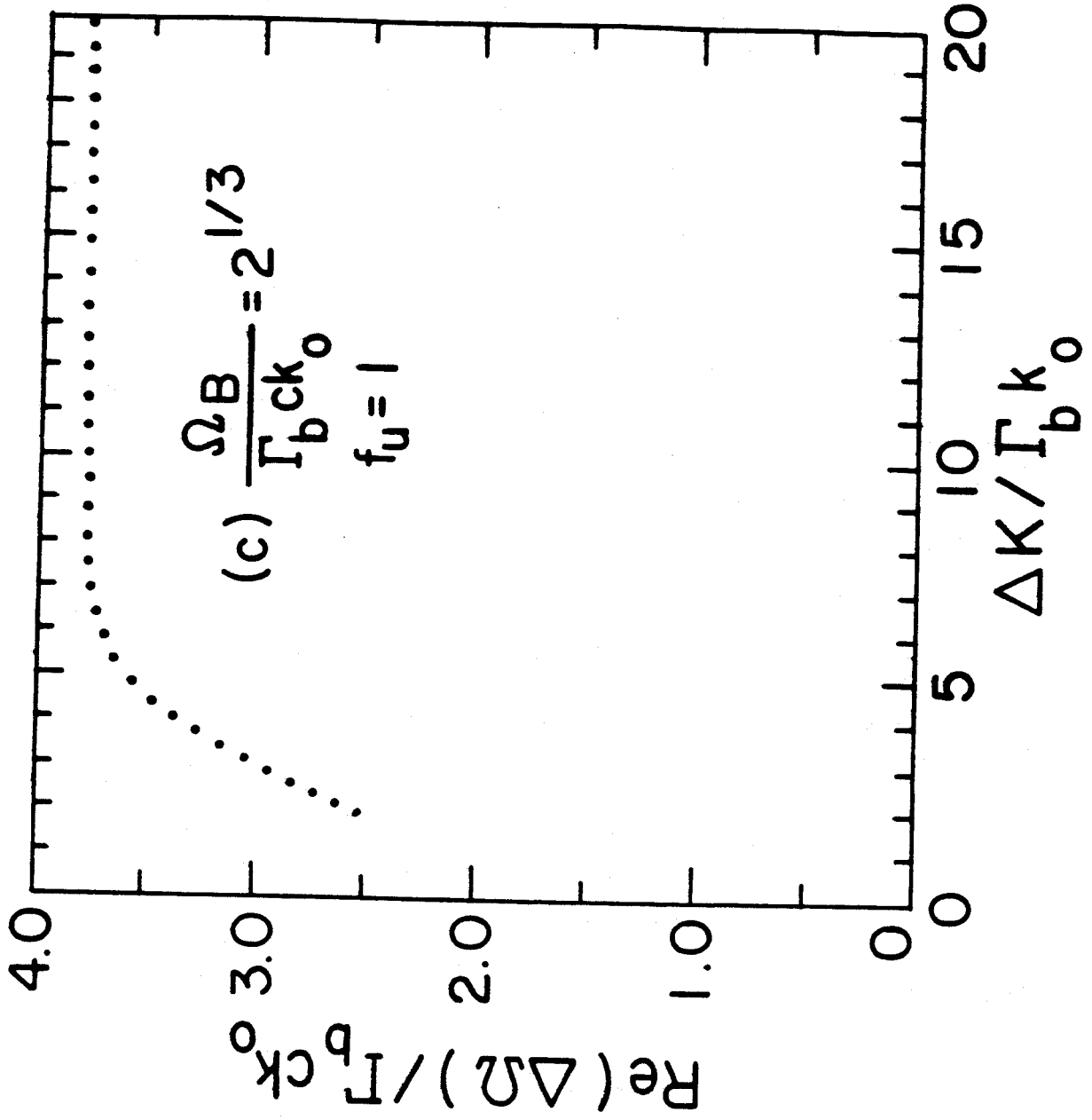
4.0
3.0
2.0
1.0
0
0
5
10
15
20
$\mathrm{Re}(\Delta\Omega)/\Gamma_b ck_o$
$\Delta K/\Gamma_b k_o$
(c) $\frac{\Omega_B}{\Gamma_b ck_o}=2^{1/3}$
$f_u=1$

Fig. 5(c)

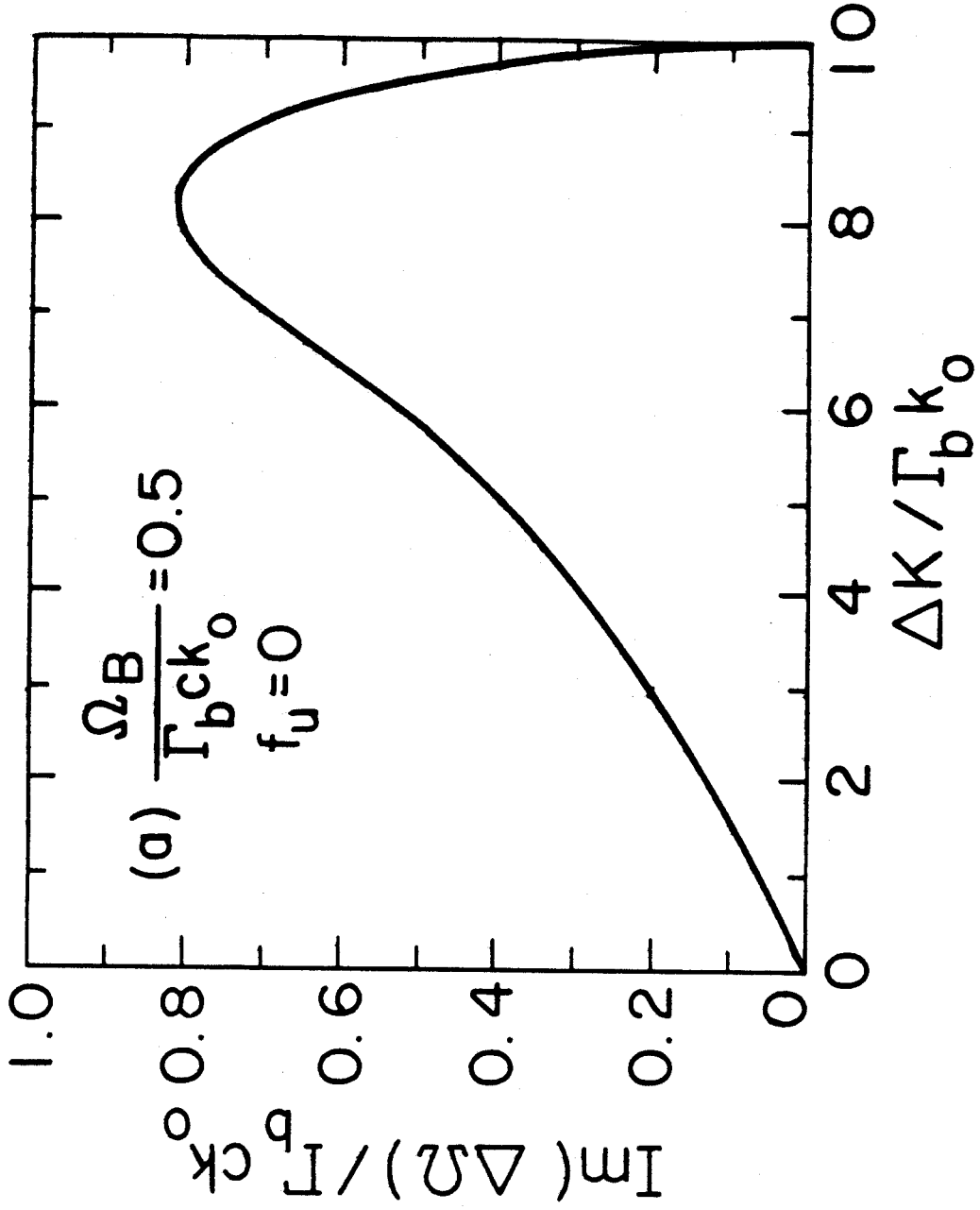
(a) $\frac{\Omega_B}{\Gamma_b c k_o}=0.5$
$f_u=0$
$\mathrm{Im}(\Delta\Omega)/\Gamma_b c k_o$
$\Delta K/\Gamma_b k_o$
0
0.2
0.4
0.6
0.8
1.0
0
2
4
6
8
10

Fig. 6(a)

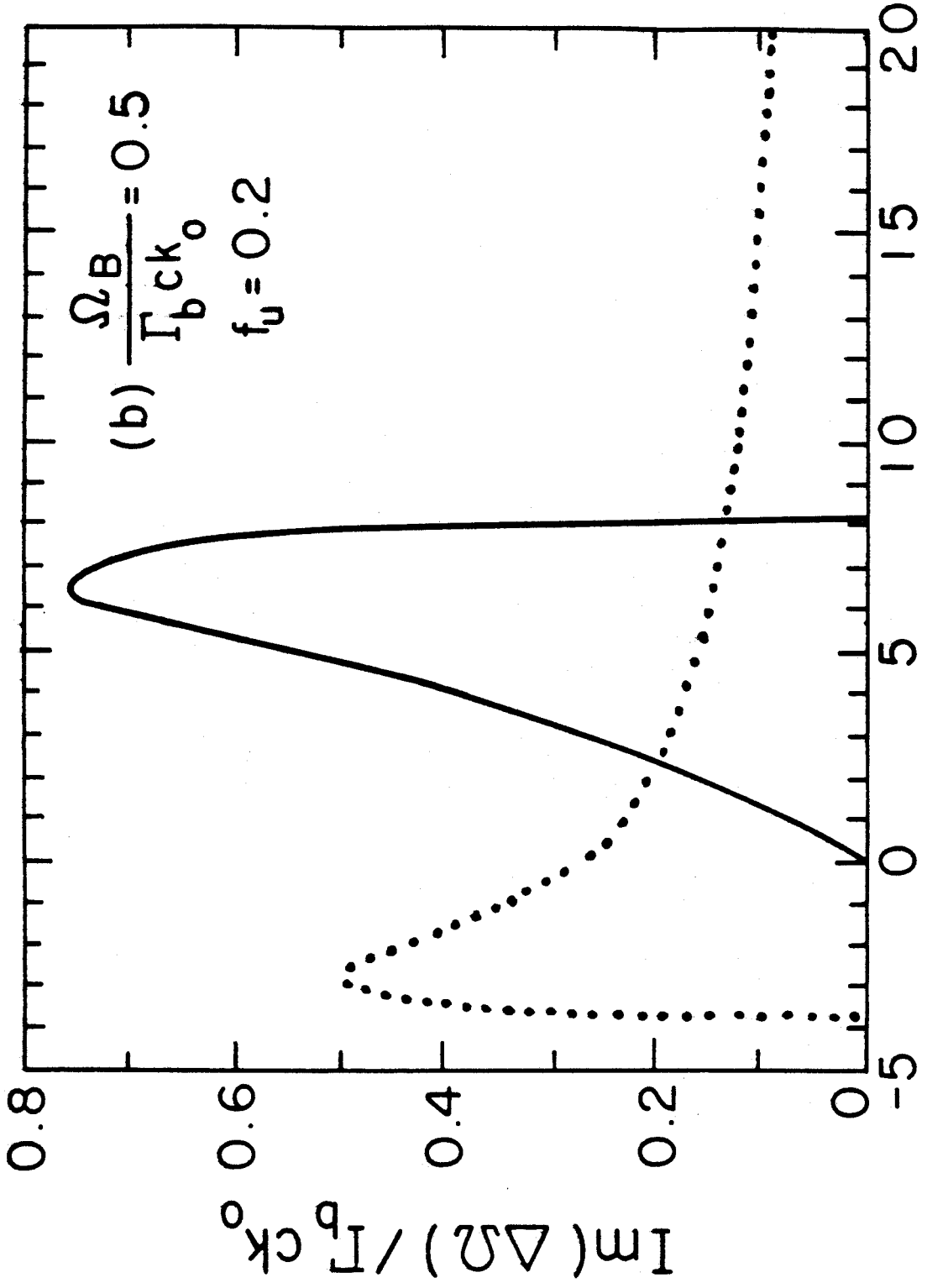
(b) $\frac{\Omega_B}{\Gamma_b c k_o} = 0.5$
$f_u = 0.2$
$\mathrm{Im}(\Delta\Omega)/\Gamma_b c k_o$
$\Delta K / \Gamma_b k_o$
0.8
0.6
0.4
0.2
0
-5
0
5
10
15
20

Fig. 6(b)

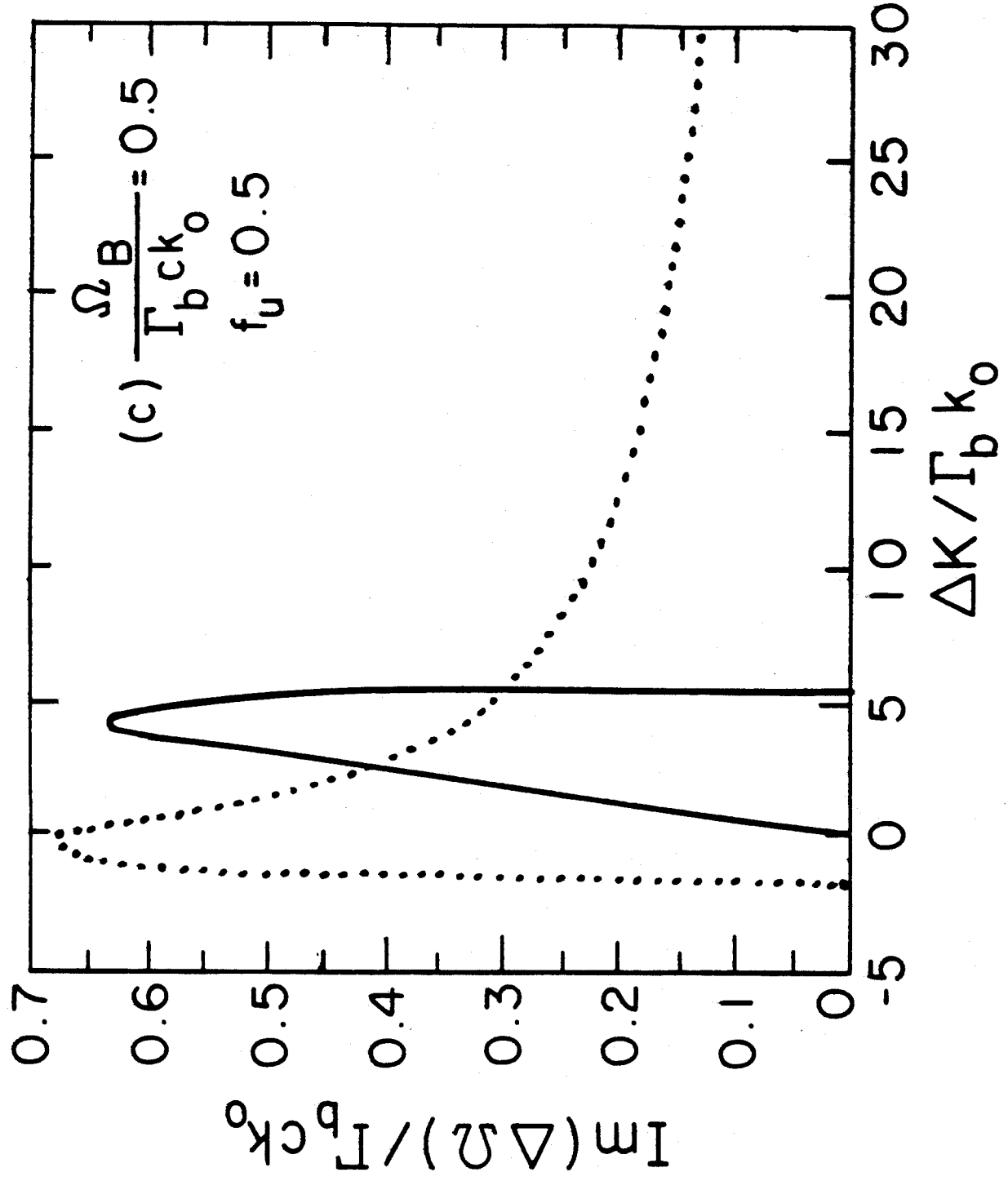
(c) $\frac{\Omega_B}{\Gamma_b c k_o} = 0.5$
$f_u = 0.5$
$\mathrm{Im}(\Delta\Omega)/\Gamma_b c k_o$
$\Delta K/\Gamma_b k_o$
0.7
0.6
0.5
0.4
0.3
0.2
0.1
0
-5
0
5
10
15
20
25
30

Fig. 6(c)

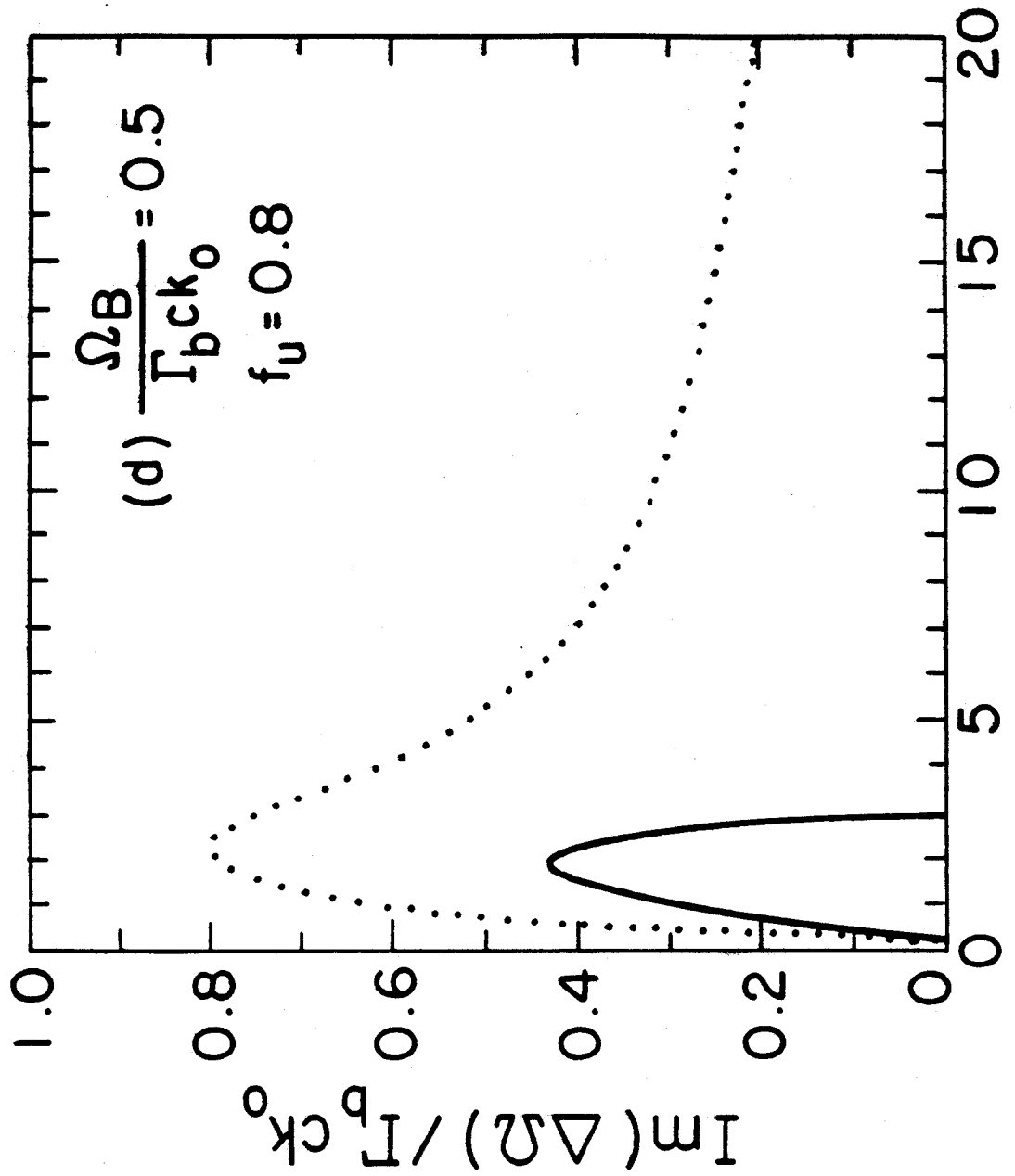
(d) $\frac{\Omega_B}{\Gamma_b c k_o} = 0.5$
$f_u = 0.8$
$\mathrm{Im}(\Delta\Omega)/\Gamma_b c k_o$
$\Delta K/\Gamma_b k_o$
0
0.2
0.4
0.6
0.8
1.0
0
5
10
15
20

Fig. 6(d)

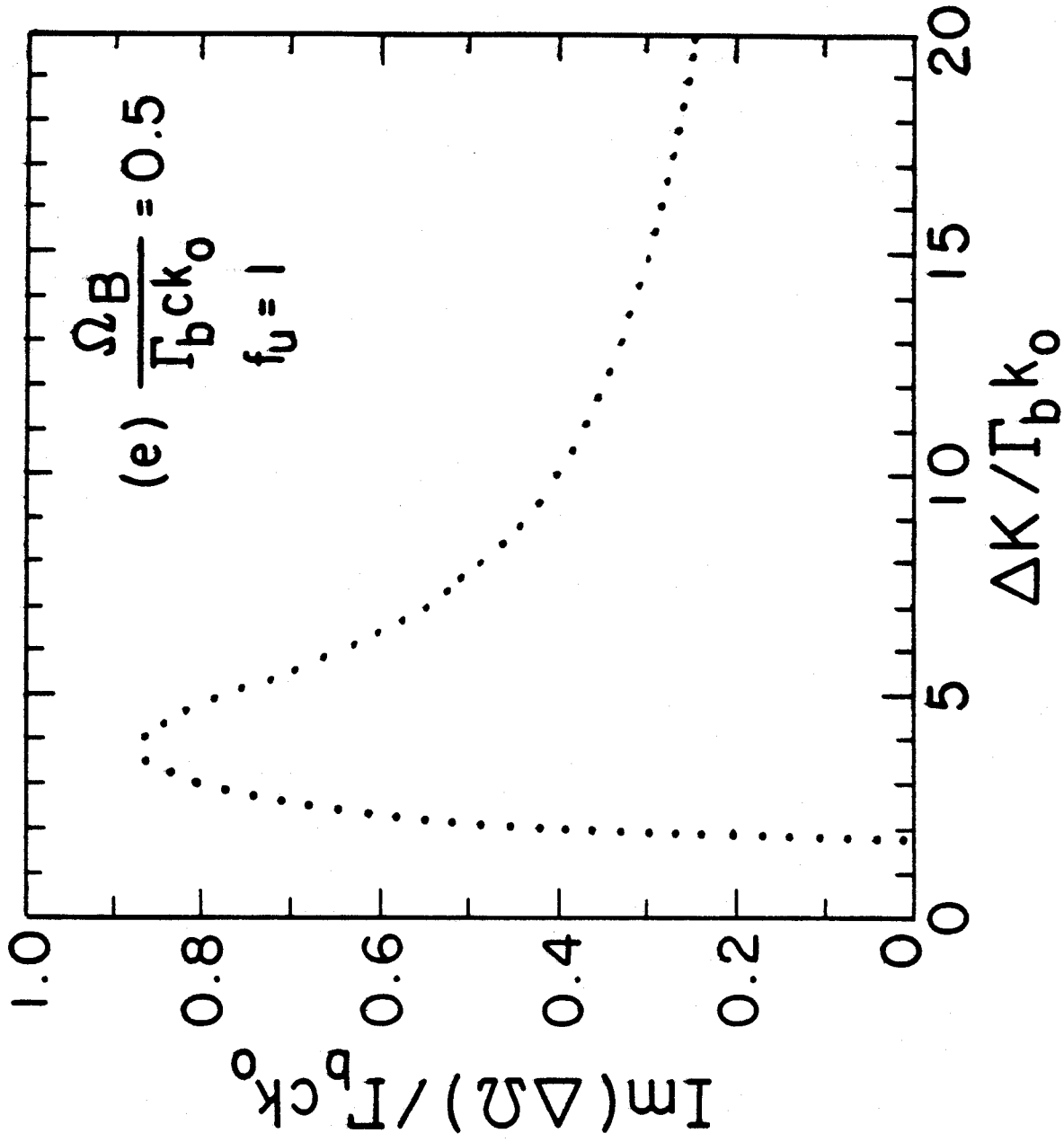
(e) $\frac{\Omega_B}{\Gamma_b c k_o} = 0.5$
$f_u = 1$
$\mathrm{Im}(\Delta\Omega)/\Gamma_b c k_o$
$\Delta K/\Gamma_b k_o$
0
0.2
0.4
0.6
0.8
1.0
5
10
15
20

Fig. 6(e)

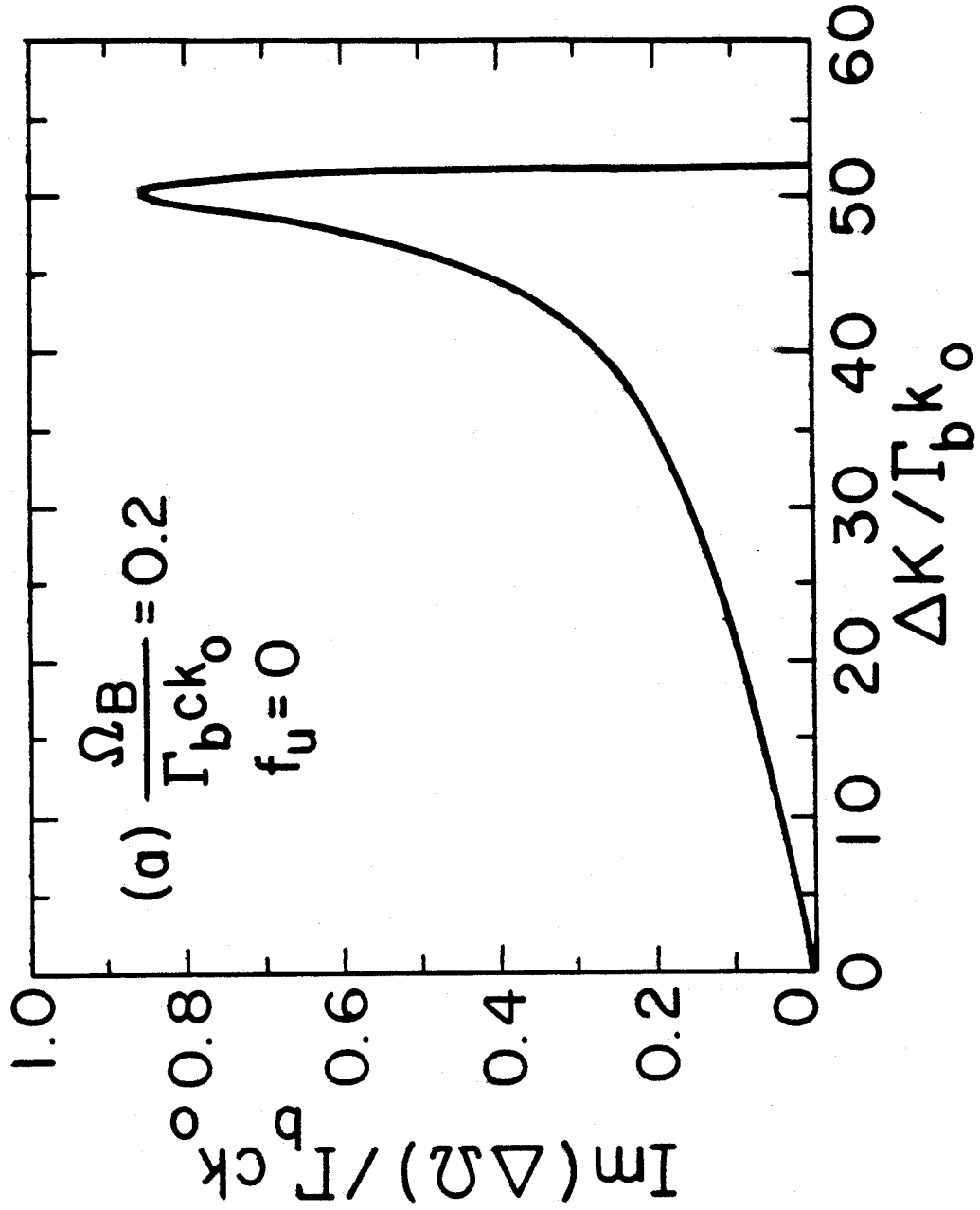
(a) $\frac{\Omega_B}{\Gamma_b c k_o} = 0.2$
$f_u = 0$
$\mathrm{Im}(\Delta\Omega)/\Gamma_b c k_o$
$\Delta K/\Gamma_b k_o$
0
0.2
0.4
0.6
0.8
1.0
0
10
20
30
40
50
60

Fig. 7(a)

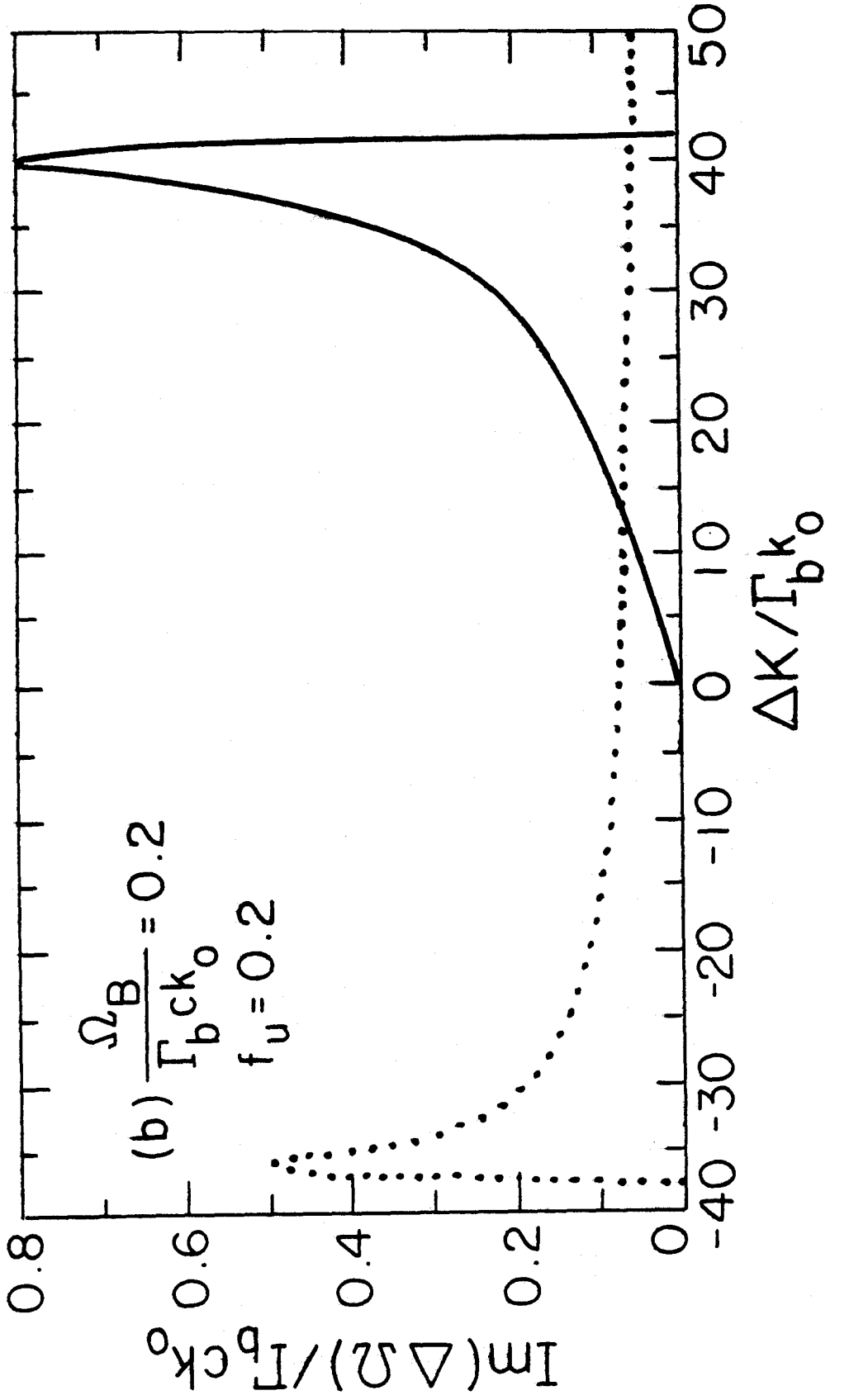
Im(ΔΩ)/Γbck0
0.8
0.6
0.4
0.2
0
-40 -30 -20 -10 0 10 20 30 40 50
ΔK/Γbk0
(b) ΩB/Γbck0 = 0.2
fu=0.2

Fig. 7(b)

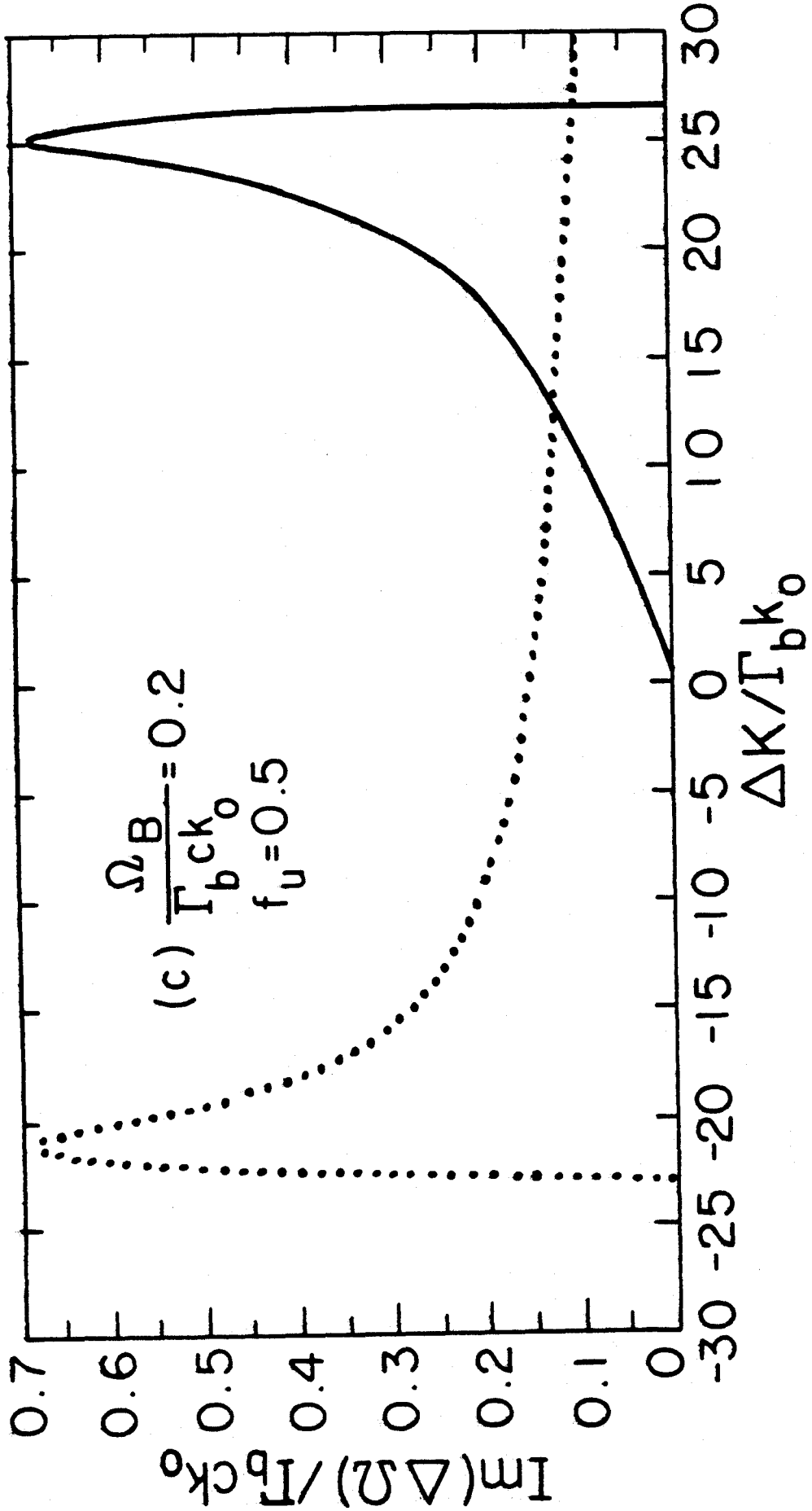
(c) $\frac{\Omega_B}{\Gamma_b c k_o} = 0.2$
$f_u = 0.5$
$\mathrm{Im}(\Delta\Omega)/\Gamma_b c k_o$
$\Delta K/\Gamma_b k_o$
0.7
0.6
0.5
0.4
0.3
0.2
0.1
0
-30
-25
-20
-15
-10
-5
0
5
10
15
20
25
30

Fig. 7(c)

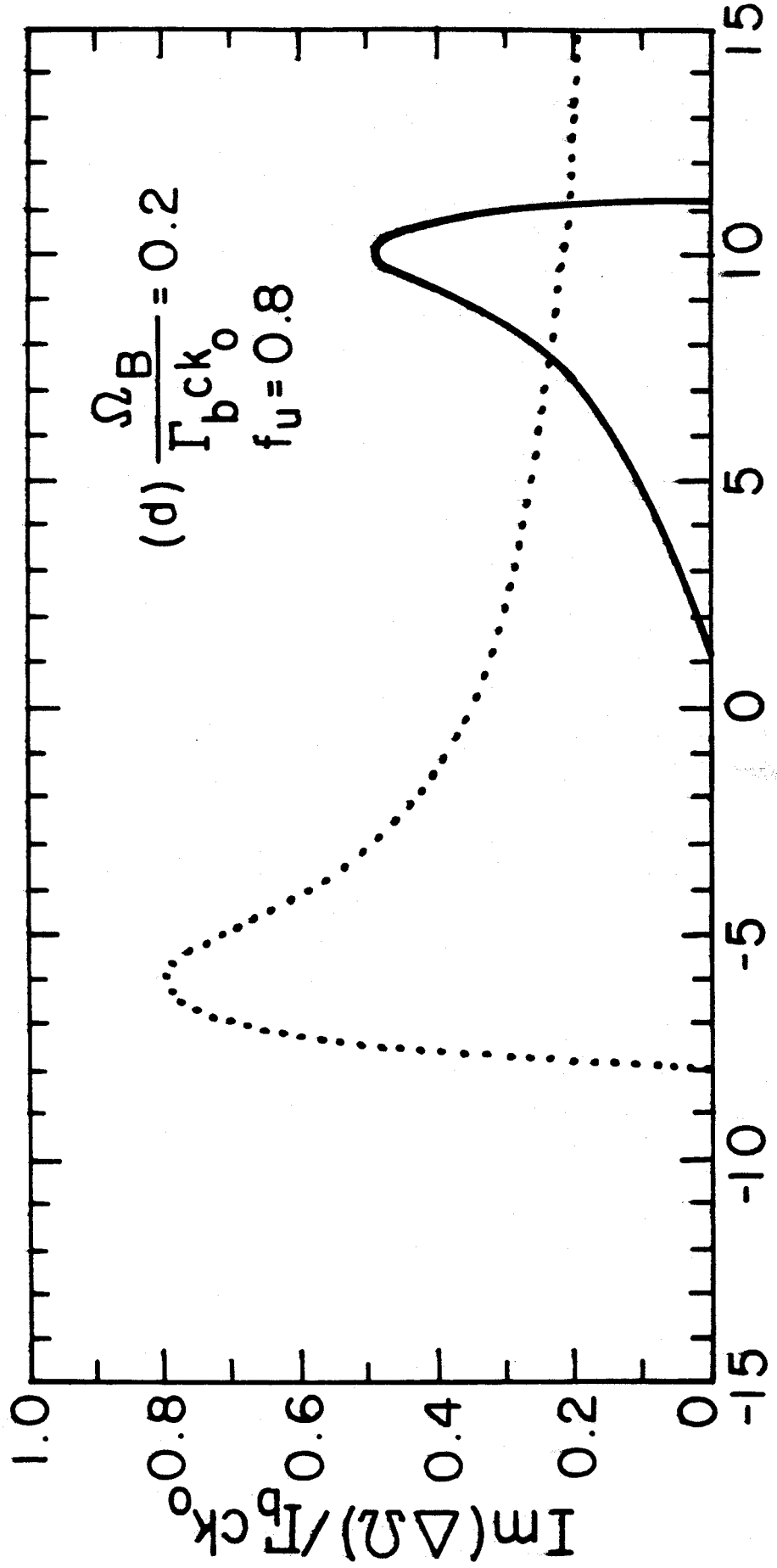
(d) $\frac{\Omega_B}{\Gamma_b c k_o} = 0.2$
$f_u = 0.8$
$\mathrm{Im}(\Delta\Omega)/\Gamma_b c k_o$
$\Delta K/\Gamma_b k_o$
1.0
0.8
0.6
0.4
0.2
0
-15
-10
-5
0
5
10
15

Fig. 7(d)

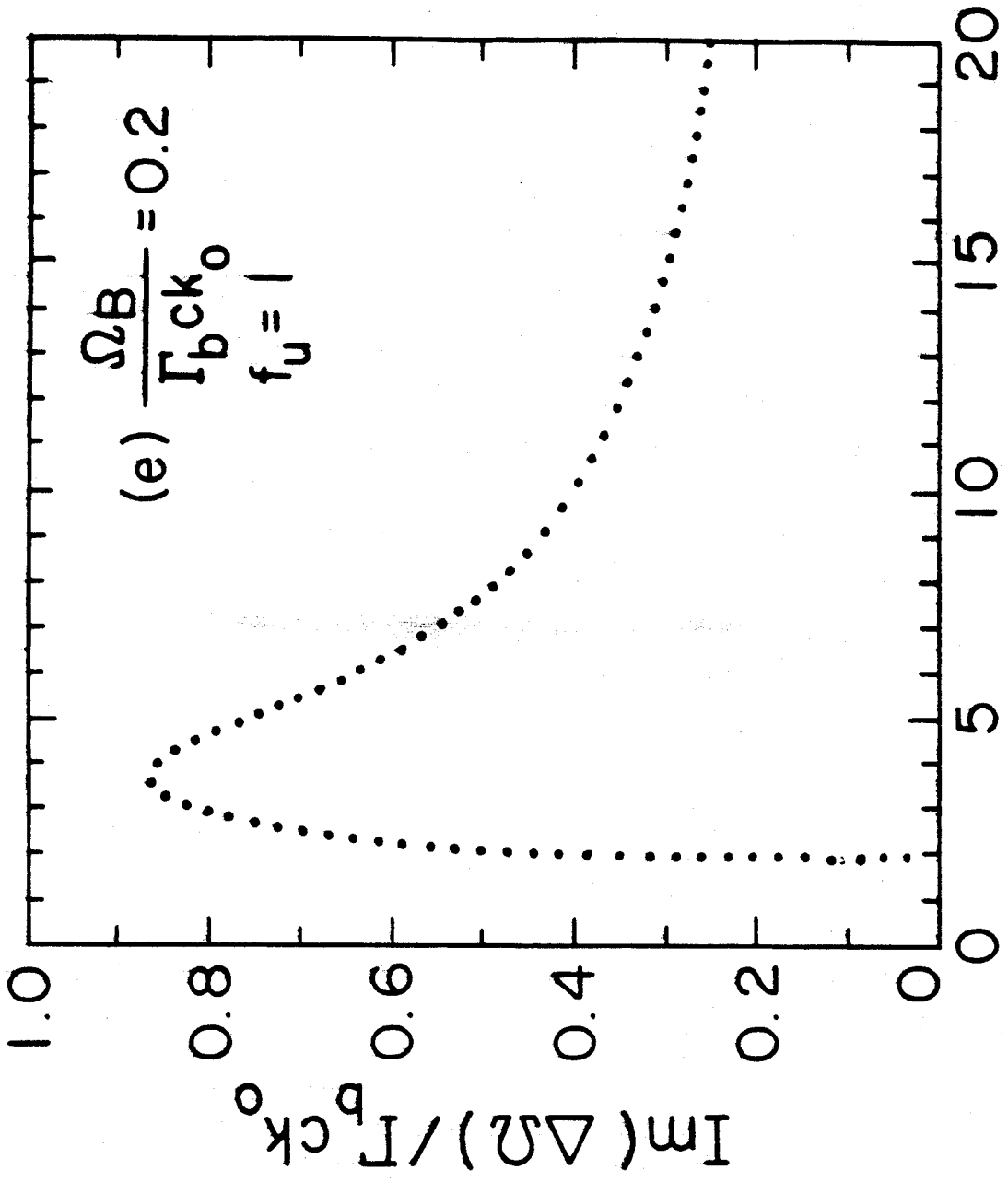
(e) $\frac{\Omega_B}{\Gamma_b c k_o} = 0.2$
$f_u = 1$
$\mathrm{Im}(\Delta\Omega)/\Gamma_b c k_o$
$\Delta K / \Gamma_b k_o$
0
0.2
0.4
0.6
0.8
1.0
0
5
10
15
20

Fig. 7(e)

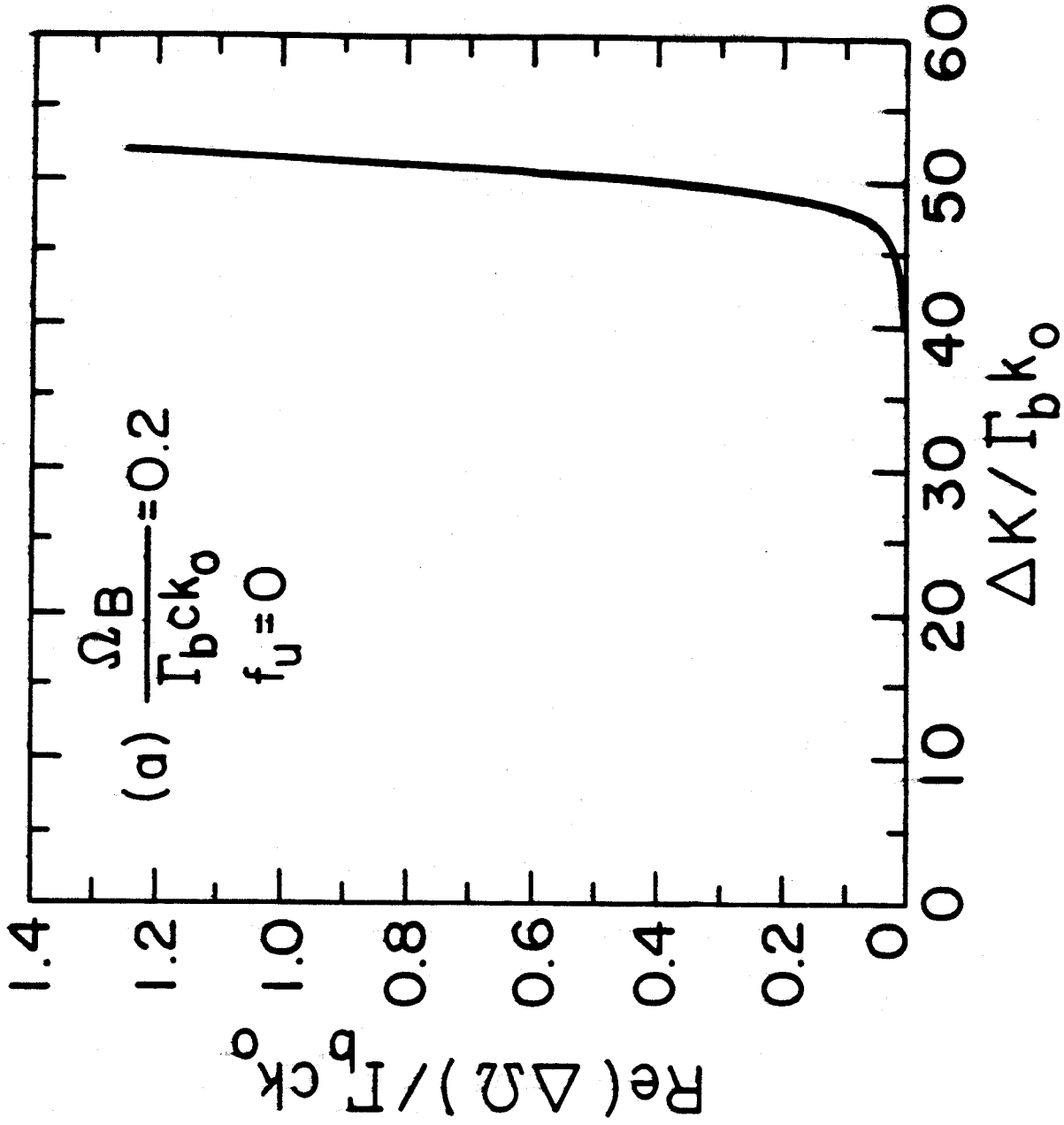
(a) $\frac{\Omega_B}{\Gamma_b c k_o}=0.2$
$f_u=0$
$\mathrm{Re}(\Delta\Omega)/\Gamma_b c k_o$
$\Delta K/\Gamma_b k_o$
0
0.2
0.4
0.6
0.8
1.0
1.2
1.4
0
10
20
30
40
50
60

Fig. 8(a)

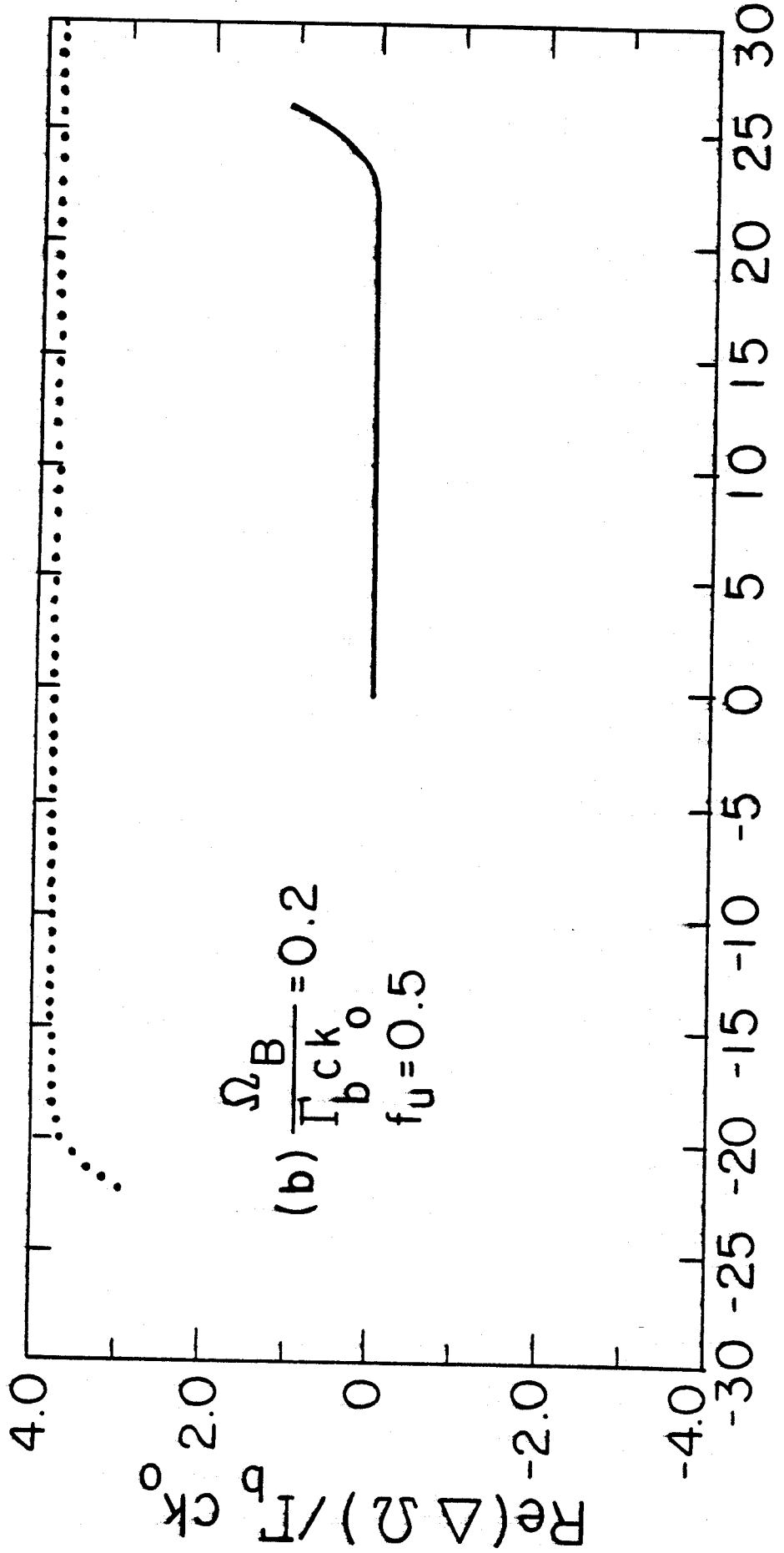
4.0
2.0
0
-2.0
-4.0
-30 -25 -20 -15 -10 -5 0 5 10 15 20 25 30
$\Delta K/\Gamma_b k_o$
$Re(\Delta\Omega)/\Gamma_b ck_o$
(b) $\frac{\Omega_B}{\Gamma_b ck_o}=0.2$
$f_u=0.5$

Fig. 8(b)

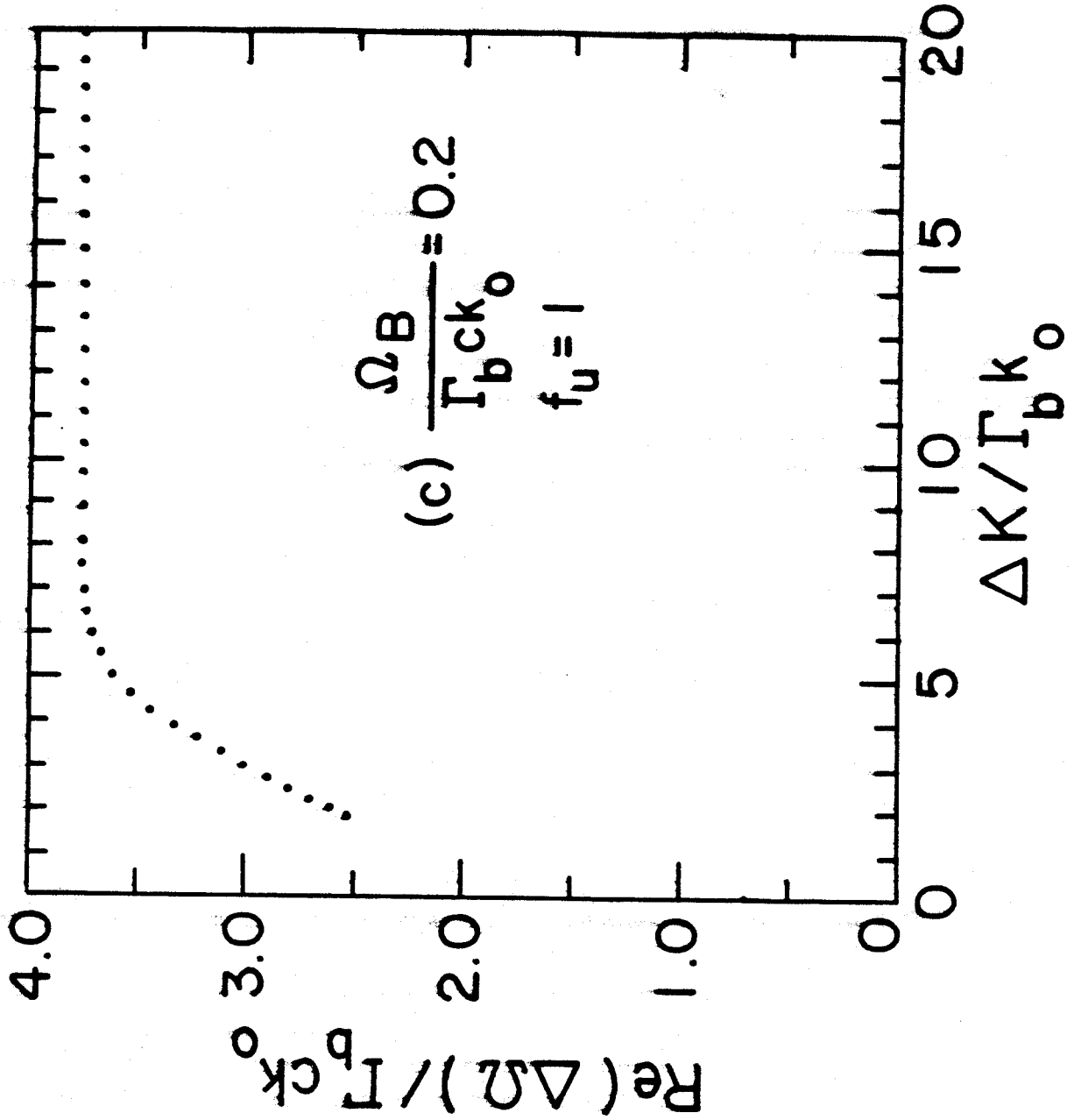
(c) $\frac{\Omega_B}{\Gamma_b c k_o} = 0.2$
$f_u = 1$
$\mathrm{Re}(\Delta\Omega)/\Gamma_b c k_o$
$\Delta K/\Gamma_b k_o$
0
1.0
2.0
3.0
4.0
0
5
10
15
20

Fig. 8(c)